Xin as a Novel Regulator of Mitochondrial Morphology and Bioenergetics in Skeletal Muscle

Molly Gingrich

A thesis submitted to the School of Graduate Studies

in partial fulfilment of the requirements for the degree

Master of Science

McMaster University, Hamilton, ON, Canada

McMaster University MASTER OF SCIENCE (2018) Hamilton, Ontario (Medical Science)

TITLE: Xin as a novel regulator of mitochondrial morphology and bioenergetics in skeletal muscle

AUTHOR: Molly A. Gingrich, HBSc. (University of Guelph)

SUPERVISOR: Dr. Thomas J. Hawke

Number of Pages: ix, 74

Abstract

Xin is a striated muscle specific, cytoskeletal adaptor protein that our lab has recently localized to the mitochondria and peri-mitochondrial regions of skeletal muscle. Further, we have identified mild mitochondrial structural and functional impairments in the skeletal muscle of Xin-/- mice. The objective of this study was to investigate the physiological effects of Xin deficiency in combination with the metabolic stress of a high fat diet, as well as the impact on skeletal muscle mitochondrial structure and function. Wild-type (WT) and Xin knockout (Xin-/-) mice were fed a high-fat diet (HFD- 60%kcal fat) for 8 weeks. HFD-fed Xin-/- mice did not gain greater body or fat mass relative to WT mice. However, Xin-/- mice had increased fasted blood glucose levels (Xin-/-: 15.8±1.042, WT: 10.7±0.652; $p<0.05$) and reduced glucose tolerance (AUC Xin-/-: 51.4±1.7, WT: 31.1±3.1; $p<0.05$) after 8 weeks of HFD feeding. Electron microscopy analysis revealed an ~1.5-fold (46.4%±7.5; $p<0.05$) increase in intermyofibrillar mitochondrial content and a ~2.8-fold (186.3%±9.6; $p<0.05$) increase in size, associated with mitochondrial swelling, streaming and loss of cristae. Complex I and complex II supported respiration were also impaired when corrected to mitochondrial content (complex I: JO_2 Xin-/-: 130.7±22.3, WT: 210.2±38.8; $p<0.05$; complex II: JO_2 Xin-/-: 124.4±13.9, WT: 175.6±20.9; $p<0.05$). We observed no changes to the protein content of either the autophagic proteins p62 or LC3, or the mitochondrial fission proteins Drp1 or Fis1 or fusion proteins Mfn1 or Mfn2. Overall, Xin-/- mice exhibited abnormal muscle mitochondrial morphology, decreased mitochondrial respiration and dysregulated glucose handling, independent of changes in body weight. Future studies are needed to identify Xin-specific binding partners and determine if Xin may be an unidentified contributor to mitochondrial myopathy and the development of metabolic disorders.

Acknowledgements

Thank you, first, to my supervisor Dr. Thomas Hawke for all of your support and guidance over the past two years. Thank you for taking a chance on me and for encouraging me every step of the way.

Thank you to my committee, Dr. Mark Tarnopolsky and Dr. Vladimir Ljubicic, for your advice and encouragement throughout my degree.

Thank you to all of the members of the Hawke and Steinberg labs for making the lab such a great place to work. Irena and Sam, thank you for going out of your way to help me throughout my first year. Dhuha, thank you for teaching me all about the Xin project. Athan and Cynthia, thank you for helping me with everything from preparing for presentations, to running experiments or just taking the time to talk.

Thank you to the undergrads who helped with this project – Ananya Sharma, Grace Martin and Rimsha Chattha. Ananya, as my first undergrad, I think that I learnt more from you than you did from me. Thank you for your dedication to this project and for your enthusiasm for stains! Grace and Rimsha, thank you for the time you have spent on Xin over the past few months. I look forward to seeing what we can discover in the year ahead.

Finally, thank you to my parents, Grant and Sandy, and my brother, Scott, for your never-ending support.

Table of Contents

List of Figures

Review of Literature

Manuscript

Appendix

List of Abbreviations

ATP – adenosine triphosphate
CAT – carnitine-acylcarnitine translocase
CoA – coenzyme A
CPTI – carnitine palmitoyltransferase I
CPTII – carnitine palmitoyltransferase II
DAG – diacylglycerol
ECM – extracellular matrix
EM – electron microscopy
ETC – electron transport chain
$FADH_2$ – flavin adenine dinucleotide
GLUT4 – glucose transport
HFD – high fat diet
IMCL – intramyocellular lipid
IMF – intermyofibrillar mitochondria
IMM – inner mitochondrial membrane
IR – insulin resistance
IRS1/2 – insulin receptor substrate 1/2
LCFA – long-chain fatty acid
MCU – mitochondrial calcium uniporter
MFN1 – mitofusin 1
MFN2 – mitofusin 2
mHCX - H^+/Ca^{2+} exchanger
mNCX - Na^+/Ca^{2+} exchanger
MTJ – myotendinous junction
NADH – nicotinamide adenine dinucleotide
NRF-1/2 - nuclear respiratory factor-1/2
OMM – outer mitochondrial membrane
OXPHOS – oxidative phosphorylation
PDK - 3-phosphoinositide-dependent protein kinase 1
PI3K - phosphatidylinositol 3-kinase
PIP_2 - phosphatidylinositol 4,5-bisphosphate
PIP_3 - phosphatidylinositol (3,4,5)-triphosphate
PINK1 – PTEN-induced putative kinase 1
PKC – protein kinase C
PGC-1α - Peroxisome-proliferator-activated receptor γ co-activator-1α
PTP – permeability transition pore
ROS – reactive oxygen species
SH3 – Src homology 3
SR – sarcoplasmic reticulum
SS – subsarcolemmal mitochondria
T2D – type 2 diabetes
TCA cycle – tricarboxylic acid cycle
TOM – translocase of the outer membrane
VDAC – voltage-dependent anion channe

Review of Literature

1. Skeletal muscle

a. Skeletal muscle in movement and metabolism

i. Introduction to skeletal muscle function

Skeletal muscle is the largest organ in the human body and is responsible for both our physical and metabolic capacities. Healthy skeletal muscle is necessary for the performance of strenuous physical activities such as weight lifting and running, but perhaps more importantly is also essential for activities of daily living such as eating, dressing and other tasks requiring simple movements. The ability to produce energy and to regulate the body's fuel sources is another key capability of this tissue. Muscle can metabolize both glucose and lipids, depending on the metabolic demand, in order to generate adenosine triphosphate (ATP) for muscle contraction and other energy dependent processes.

ii. Introduction to skeletal muscle structure

The function of skeletal muscle is dependent on its structure. Skeletal muscle is made up of individual myofibres, or muscle cells, grouped together into muscle fascicles and then bundled to form whole muscle. At the molecular level, cytoskeletal proteins are required for co-ordinated force production. Skeletal muscle contains four major groups of cytoskeletal proteins: those found in the sarcomere, the costamere, the myotendinous junction and the intermediate filaments. However, all of these structures are interconnected to allow for force transmission.

The primary contractile unit of the muscle fibre is the sarcomere. These repeated structures are bound on either side by a protein dense z-disc and contain actin thin filaments and myosin thick filaments[1]. Divisions of the sarcomere include the I-band, located on either side of

the z-disc, the A-band, running the entire length of the thick filaments, and the H-band, found at the centre of the A-band[2] (Fig. 1). As thin and thick filaments slide against each other, muscle contraction occurs and adjacent z-discs are brought closer together[1]. The principal role of the z-disc is to cross-link thin filaments of adjacent sarcomeres via the protein α-actinin[3]. However, the z-disc also acts as an anchor for a variety of proteins including titin, which is important in thick filament stabilization, and nebulin, which serves as a ruler during thin filament assembly[3]. Also within the z-disc is the protein filamin C, an important link between sarcomere and costamere structures[4].

Comparable to the focal adhesion complexes of other cell types, the costamere is found at the boundary between the cell and the extracellular matrix (ECM)[5]. It allows for bidirectional force transmission and provides a link between the sarcomere and sarcolemma, primarily through the dystrophin complex and the vinculin-talin-integrin complex, which binds to α-actinin and various ECM components such as collagen and laminin[5]. The myotendinous junction (MTJ) is similar to the costamere in its protein composition and function, as it is necessary for the transmission of force from the sarcomere to the muscle tendon[6]. Finally, intermediate filaments maintain cellular architecture and stability, primarily through the protein desmin and the structural networks it creates via its interactions with various cytoskeletal proteins[4]. For a more in depth description of muscle structure and function, please see the review by Frontera & Ochala[7].

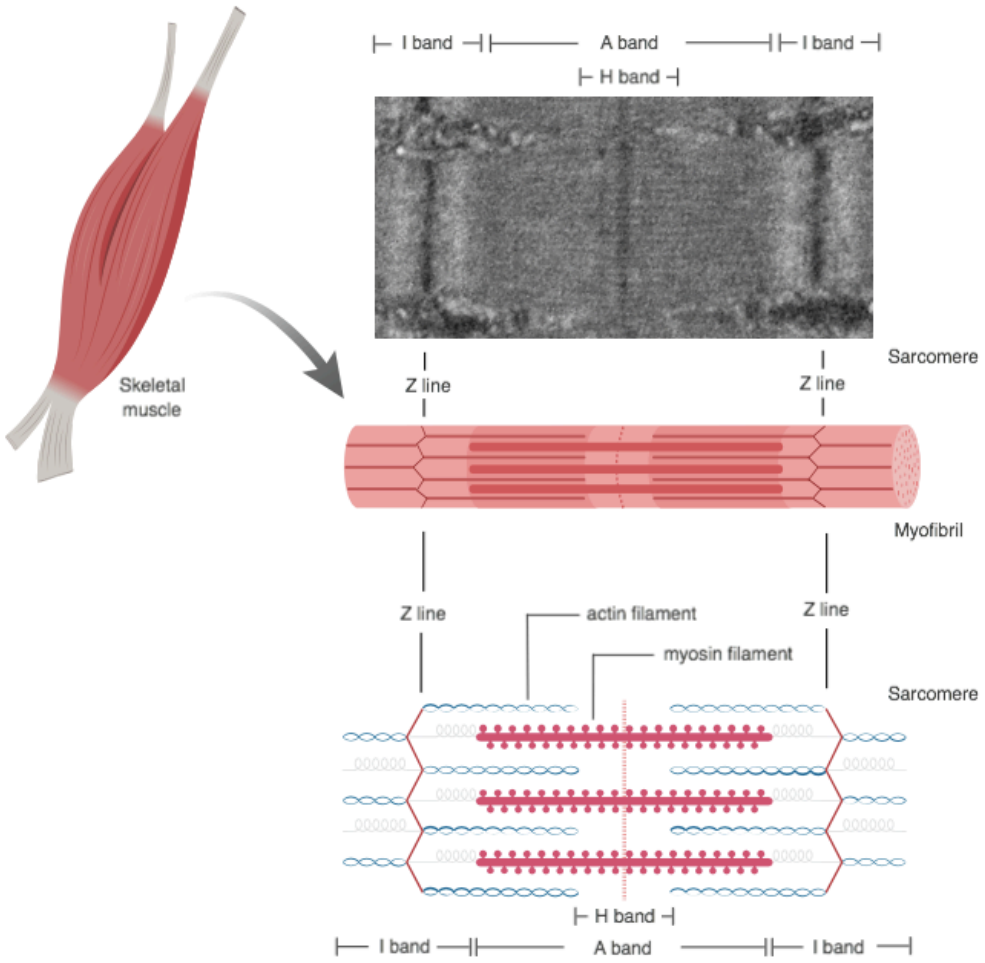

Figure 1. Skeletal muscle sarcomere structure. Skeletal muscle is composed of single muscle fibres, called myofibrils, made up of contractile units known as sarcomeres. Sarcomeres are in turn made up of myosin thick filaments and actin thin filaments, with actin filaments anchored at protein-dense z-discs defining the sarcomere borders. The sarcomere can be broken up into various bands including the I band, containing only thin filaments, the H band, containing only thick filaments, and the A band, stretching the whole length of the thick filaments.

iii. Skeletal muscle glucose and lipid metabolism

In addition to force production, skeletal muscle is also an important metabolic regulator, as various fuel sources must be broken down to create energy in the form of ATP. Skeletal muscle relies on differing fuel sources depending on the metabolic demand. For high intensity exercise, muscle is primarily dependent on glucose metabolism[8]. However, lipids are an important source of fuel both at rest and during prolonged, low intensity exercise[8].

Skeletal muscle glucose uptake is stimulated by both physical activity and insulin; a hormone secreted from the pancreas in response to post-prandial increases in blood glucose. During times of nutrient excess, glucose within muscle is converted into glycogen for storage and subsequent use during times of nutrient deficiency. Glucose or glycogen is converted into pyruvate through the process known as glycolysis, and then into acetyl-CoA, which enters the common TCA cycle/oxidative phosphorylation pathway for ATP production[9]. This process relies on the availability of oxygen. However, anaerobic glycolysis occurs under conditions of oxygen deprivation and instead converts pyruvate into lactate, again resulting in ATP production[9].

In order for lipid metabolism to occur, fatty acids brought into the cytosol of skeletal muscle from the blood and are metabolized within mitochondria. While small- and medium-chain fatty acids can pass freely into the mitochondrial matrix, long-chain fatty acids (LCFA) rely on various enzymes and transporters[10]. Within the cytosol, LCFA's are first bound to Coenzyme A (CoA) by Fatty-acyl-CoA synthase to create Fatty-acyl-CoA[11]. This molecule can pass freely through the outer mitochondrial membrane, but must be linked to carnitine via carnitine palmitoyltransferase I (CPTI) within the mitochondrial intermembrane space for transport through the inner mitochondrial membrane by carnitine-acylcarnitine translocase (CAT)[11]. Once inside the matrix, fatty acyl-CoA is regenerated through the removal of carnitine

by carnitine palmitoyltransferase II (CPTII) and enters into the beta-oxidation pathway[11]. A two-carbon segment is cleaved with each pass through the beta-oxidation cycle, resulting in the release of acetyl-CoA to again enter into the common TCA cycle/oxidative phosphorylation pathway for ATP production[11] (Fig. 2).

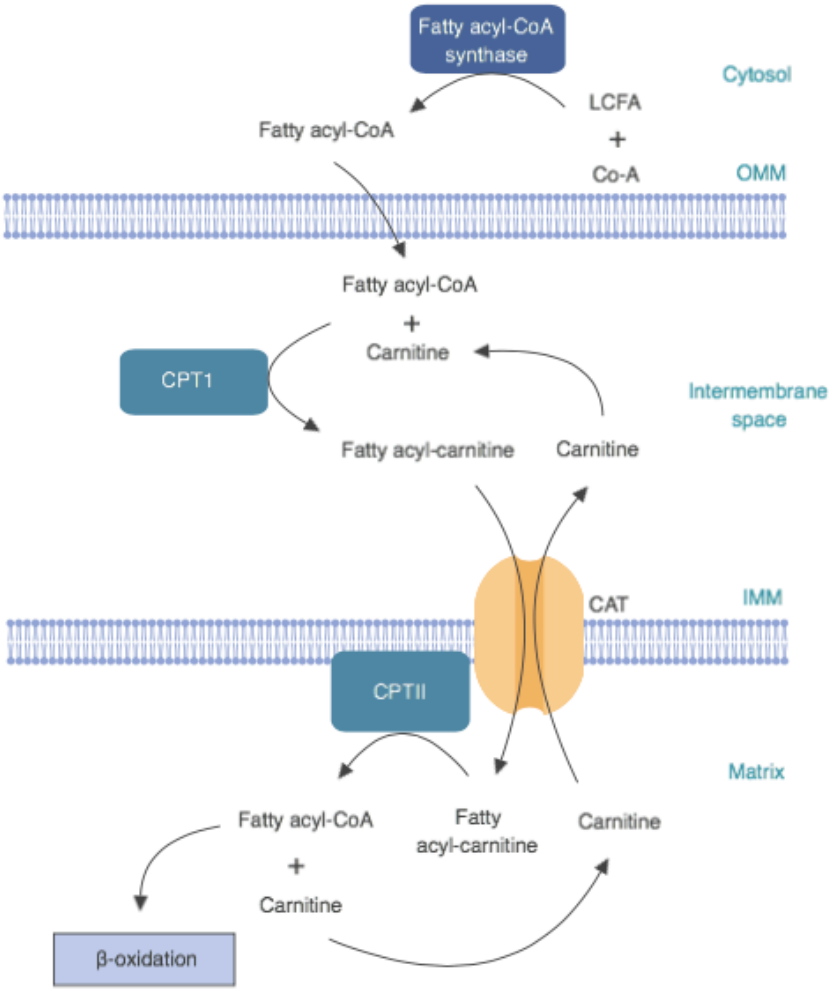

Figure 2. Mitochondrial fatty acid transport. Long chain fatty acids (LCFA) enter the cell and are quickly converted into fatty-acyl CoA by the enzyme fatty acyl-CoA synthase. Fatty acyl-

CoA crosses the outer mitochondrial membrane (OMM) freely but is bound to carnitine within the intermembrane space via carnitine palmitoyltransferase-I (CPT-I). Fatty acyl-carnitine is generated and passes through the inner mitochondria membrane (IMM) via carnitine-acylcarnitine translocase (CAT) before being converted back into fatty acyl-CoA by carnitine palmitoyltransferase-II (CPT-II) for metabolism via β-oxidation. Free carnitine is transported into the intermembrane space through CAT and bound to fatty acyl-CoA to complete the cycle.

2. Mitochondria and skeletal muscle

a. Mitochondrial physiology

i. Structure

Mitochondria are double membrane bound organelles, enclosed by both an inner and outer membrane, that primarily function to produce cellular energy in the form of adenosine triphosphate (ATP). The outer mitochondrial membrane (OMM) is composed of a phospholipid bilayer, similar to that of the cell membrane, and is considered largely permeable due to voltage-dependent anion channels (VDAC) which allow for the free diffusion of small molecules such as ions and ATP. Larger molecules, such as proteins, are transported through the OMM via the translocase of the outer membrane (TOM) complex. The inner mitochondrial membrane (IMM) is vastly impermeable and forms the major barrier between the mitochondrial matrix and the cytosol. Cristae, or membrane folds, function to increase the surface area of the IMM. The intermembrane space is located between the OMM and IMM, while the IMM encloses the mitochondrial matrix.

ii. Subpopulations

Skeletal muscle mitochondria can be divided into two subpopulations – subsarcolemmal (SS) and intermyofibrillar (IMF)[12]. These subpopulations differ in their location, morphology, function and protein composition. SS mitochondria are large with lamellar cristae while IMF mitochondria are more compact[13]. Functionally, IMF mitochondria have been shown to play a greater role in energy production[14,15]. Protein characterization has indicated that 38 of 325 identified proteins are differentially expressed between SS and IMF mitochondrial subpopulations, with IMF mitochondria having a greater number of proteins associated with oxidative phosphorylation[13]. This may provide an explanation for the finding that IMF mitochondria make up a greater proportion of total muscle mitochondrial volume compared to SS mitochondria[13].

iii. Mitochondrial Metabolism

Mitochondria are the hubs of cellular metabolism and have the ability to integrate many pathways with the metabolic state of the cell. While mitochondria are involved in various biological processes, their main function is the production of cellular energy, in the form of ATP, via the tricarboxylic acid (TCA) cycle and oxidative phosphorylation. The TCA cycle occurs in the mitochondrial matrix and integrates carbohydrate, fat and protein metabolism. The common metabolite acetyl-CoA, produced by both the glycolysis of glucose and the beta-oxidation of fatty acids, is fed into the TCA cycle. Through a series of chemical reactions, acetyl-CoA is oxidized to yield CO_2, NADH and $FADH_2$. While CO_2 is a waste product that will be released from the cell, NADH and $FADH_2$ are reducing equivalents necessary for oxidative phosphorylation[16].

Oxidative phosphorylation (OXPHOS) uses the electron transport chain (ETC) to couple the oxidation of reducing equivalents to the generation of a proton gradient that subsequently allows for the production of ATP. The ETC is made up of a series of enzymes (complexes I, II, III and IV) embedded in the IMM. Electrons are transferred down the chain from complex to complex through a series of redox reactions until the final electron acceptance at Complex IV. Here, oxygen is reduced and water is formed[16]. The energy released at each step of the chain is captured in the form of an electrochemical gradient. This occurs as the passage of electrons down the chain is coupled to the pumping of protons across the inner mitochondrial membrane, from matrix to intermembrane space, creating a store of potential energy. The flow of protons back down the gradient is coupled to ATP synthesis, as first described by Peter Mitchell's chemiosmotic hypothesis[17]. The flow of protons across the inner mitochondrial membrane through ATP synthase rotates a part of this enzyme, creating a motor to drive the energetically unfavourable phosphorylation of ADP to the high-energy molecule ATP to complete the energy generation process[16]

The process of protons entering back into the mitochondrial matrix by means other than ATP synthase is known as proton leak. This occurs via IMM uncoupling proteins, which provide a channel for proton diffusion[16]. Activation of uncoupling proteins allows protons to flow across the IMM into the matrix, bypassing ATP synthase and dissipating the electrochemical gradient. With a reduced gradient to pump against, the respiratory rate increases. However, this results in a futile cycle where energy is no longer converted into ATP but instead dissipated as heat[16]. This process is essential for non-shivering thermogenesis in small mammals, which takes place primarily in brown adipose tissue through the uncoupling protein UCP1[16]. Additional uncoupling proteins: UCP2 - predominantly expressed in the lymphoid system, macrophages and pancreatic

islets - and UCP3 - found mainly in skeletal muscle, also have important physiological functions including the regulation of insulin secretion, fatty acid metabolism and reactive oxygen species (ROS) production[18] (Fig. 3).

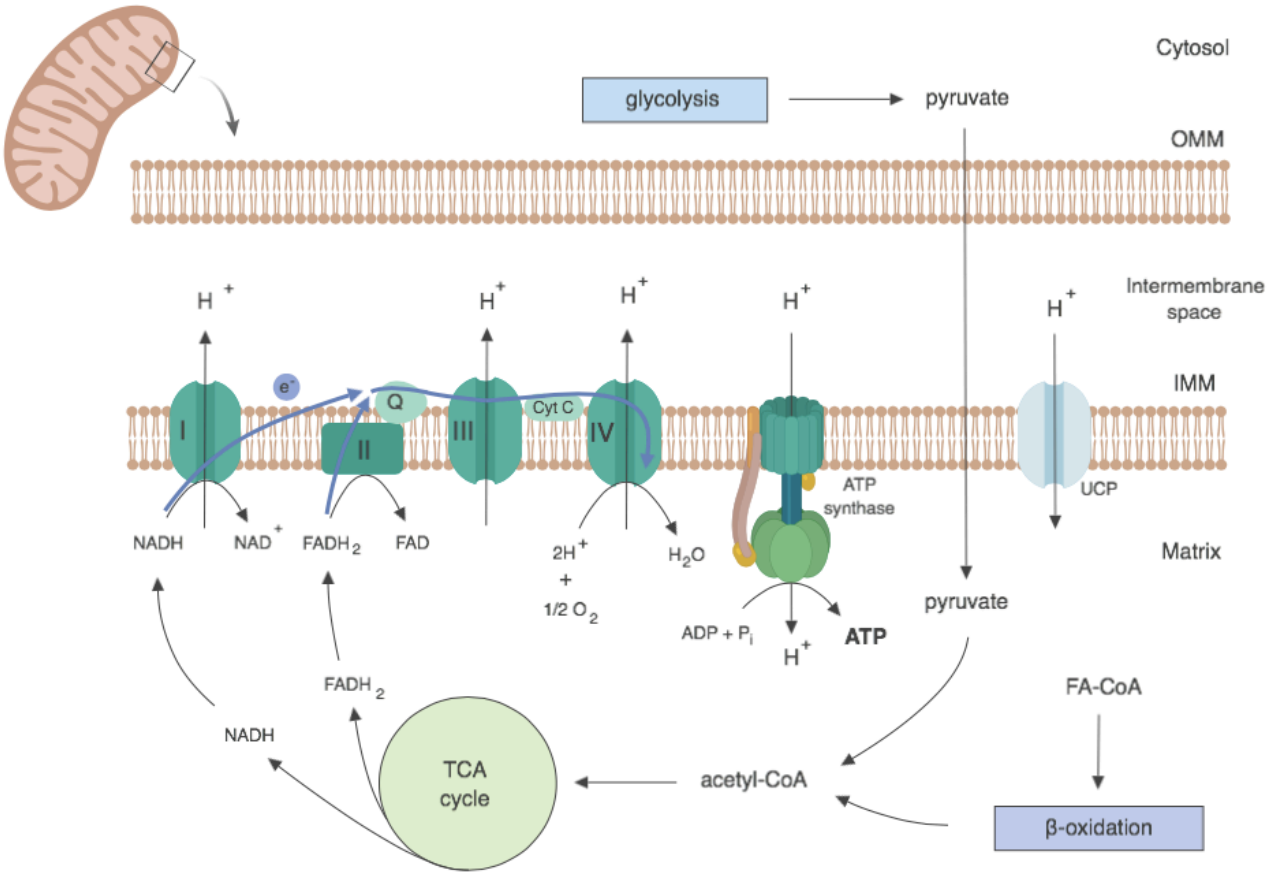

Figure 3. Mitochondrial metabolism. ATP is produced via oxidative phosphorylation in the mitochondria. Metabolism of glucose by glycolysis in the cytosol and fatty acids by β-oxidation in the mitochondrial matrix lead to the production of the metabolic intermediate acetyl-CoA. Acetyl-CoA is fed into the TCA cycle, which produces the reducing equivalents NADH and $FADH_2$ to feed into the electron transport chain (ETC) at Complex I and Complex II. Electrons

flow down the chain through a series of redox reactions that ends with the final reduction of oxygen to water. Complex I, III and IV couple these redox reactions to the pumping of protons (H^+) from the mitochondrial matrix across the inner mitochondrial membrane (IMM) into the intermembrane space to create an electrochemical gradient. The flow of protons back down the gradient into the mitochondrial matrix, through ATP synthase, drives an enzymatic motor allowing for ATP production. Under certain conditions, protons are able to bypass ATP synthase and flow back into the matrix through uncoupling proteins (UCP), generating heat but creating a futile cycle.

iv. ROS Generation

In addition to proton leak, mitochondria also experience electron leak. The generation of reactive oxygen species (ROS) occurs when electrons escape from the respiratory chain at any point prior to the final reduction of oxygen, most commonly at complexes I and III[19]. These lost electrons are highly unstable and react with oxygen to produce superoxide radical, which is subsequently converted into other ROS species such as hydroxyl radical and hydrogen peroxide[19]. Increased electron leak is associated with a decreased respiratory rate, as a faster respiratory rate favours the transfer of electrons to oxygen at complex IV.

Superoxide radical and ROS species generated by electron leak were once thought to have only pathological effects. However, recent research has shown that ROS are necessary for physiological cellular functions as well, with the distinction between a physiological or pathological outcome determined by the level of ROS within the cell. A mild cellular stress induces a mild increase in ROS and allows for cellular adaptation and survival. For example,

hypoxia induces an increase in H_2O_2 to activate the transcription factor hypoxia-inducible factor 1 and upregulates genes necessary to adapt to this altered environment[20]. On the other hand, a severe stressor such as radiation induces a greater increase in ROS and can lead to apoptosis[21]. ROS also act as key signaling molecules in pathways such as stem cell differentiation and inflammation[22].

To keep ROS levels relatively low under physiological conditions, mitochondria have several antioxidant defenses including glutathione, superoxide dismutase and catalase[22]. An additional method of ROS control occurs through a negative-feedback loop created by ROS themselves. High levels of ROS activate uncoupling proteins, permitting the flow of protons back into the matrix and dissipating the electrochemical gradient. As the respiratory rate increases, electron transfer to oxygen is favoured, electron leak and ROS production decrease, and activation of uncoupling proteins ends[19].

v. Calcium Handling

The same electrochemical gradient that drives the flow of protons into the matrix also drives an influx of calcium. Differences in both charge and calcium concentration between the intermembrane space and the mitochondrial matrix permits the passive movement of calcium through the inner mitochondrial membrane via the mitochondrial calcium uniporter (MCU)[23]. Under physiological conditions, the concentration of calcium in the matrix remains low through the action of efflux pumps, including the Na^+/Ca^{2+} exchanger (mNCX) and the H^+/Ca^{2+} exchanger (mHCX)[24]. One role of calcium within the mitochondria is the regulation of metabolism, as it upregulates the activity of three TCA cycle matrix dehydrogenases to increase the production of reducing equivalents for the respiratory chain[16].

Under physiological conditions, cytosolic calcium concentrations are kept relatively low. This, in combination with the MCU's low affinity for calcium, means that mitochondria must take advantage of calcium microdomains to facilitate calcium flux[24]. Mitochondria are often located adjacent to the sarcoplasmic reticulum (SR), where Ca^{2+} release will create a microdomain of high $[Ca^{2+}]_c$ which meets the low affinity requirements of the MCU and permits calcium flow into the matrix[24].The high calcium concentration quickly dissipates following the influx, inhibiting further transport through the MCU and preventing both Ca^{2+} overload in the matrix and cycling across the membrane[24].

vi. Biogenesis

Mitochondrial biogenesis, or the generation of new mitochondria from the existing mitochondrial pool, can be stimulated by a number of factors including exercise, cold exposure and oxidative stress[25]. These factors activate the master regulator of mitochondrial biogenesis, peroxisome-proliferator-activated receptor γ co-activator-1α (PGC-1α), which upregulates the transcription of mitochondrial proteins by binding to various transcription factors [25]. Two of these transcriptions factors, nuclear respiratory factor-1 and -2 (NRF-1, NRF-2), upregulate the transcription of mitochondrial transcription factor A (Tfam), which then travels to the mitochondria to activate the transcription of mtDNA[26]. The resulting increased expression of both nuclear and mitochondrial encoded proteins allows for the generation of new mitochondria.

In addition to the transcriptional control of mitochondrial biogenesis, mitochondria rely on fission, fusion and mitophagy to maintain a healthy mitochondrial network within the cell. Fusion occurs when two mitochondria combine and can rescue partially damaged mitochondria through the mixing of mitochondrial contents. Fusion between a damaged and healthy

mitochondrion allows for compensation by functional components, so long as the mitochondrion's mutation load remains below 80-90%[27]. Mitochondrial fusion relies on interactions between the dynamin-related GTPases mitofusin-1 and -2 (Mfn1, Mfn2), both embedded within the OMM[28]. Once the outer membranes of two adjacent mitochondria have fused, the process is completed through the fusion of the inner membranes, mediated by the protein Opa1[28].

Contrary to fusion, fission involves the separation of a mitochondrion into two parts. In response to higher metabolic demand, fission functions to increase mitochondrial content. However, this process also provides a means of quality control, as the asymmetrical sorting of mitochondrial proteins and the unequal separation into two daughters, mediated by the fission proteins Drp1 and Fis1, allows for the segregation and subsequent degradation of damaged mitochondrial components[28,29]. Removal of damage creates a healthy mitochondrion which can function normally, while retention of damage within the other daughter results in a loss of membrane potential and elimination via mitophagy.

Mitophagy maintains a healthy mitochondrial network by removing damaged mitochondria in which the membrane potential has been reduced below a critical threshold[30]. This process is controlled by the kinase PTEN-induced putative kinase 1 (PINK1). Under physiological conditions, PINK1 is transported from the cytosol into the IMM, where it is degraded by presenilins-associated rhomboid-like protein (PARL) to keep PINK1 expression low[28]. However, a loss of membrane potential prevents PINK1 import and degradation, resulting in the accumulation of PINK1 on the OMM and recruitment of the E3 ligase Parkin from the cytosol[28]. Parkin then ubiquinates various proteins found on the OMM, now tagging the damaged mitochondria for degradation and causes the recruitment of autophagic machinery[28]. In

this way, mitophagy allows for the selective tagging and degradation of damaged mitochondria while preserving functional mitochondria within the mitochondrial pool.

vi. Apoptosis

Mitochondria also play an important role in programmed cell death, or apoptosis. Cellular apoptosis can be activated through two different pathways: 1) the extrinsic pathway - which is initiated by the binding of various "death factors" to cell membrane receptors, and 2) the mitochondrial-mediated intrinsic pathway[21]. The intrinsic pathway can be initiated by a variety of non-receptor mediated cellular stresses such as radiation or ROS accumulation[21]. These stimuli are common in their ability to induce the opening of the mitochondrial permeability transition pore (PTP), located in the IMM, which causes the loss of inner membrane potential, the flow of H_2O into the matrix, mitochondrial swelling and subsequent rupture of the OMM[21]. Pro-apoptotic factors located within the IMS, such as cytochrome c and apoptosis inducing factor, are released into the cytosol and activate various caspase signaling cascades resulting in apoptosis[21].

b. Mitochondria and skeletal muscle health

i. Mitochondrial myopathy

As previously described, mitochondria are essential for fuel metabolism and energy production within skeletal muscle. Impairments to skeletal muscle mitochondria, either structural or functional, can result in mitochondrial myopathy, or mitochondria-associated muscle disease[31]. Mutations to either mitochondrial genes or nuclear genes which code for mitochondrial proteins can be acquired or spontaneous[32]. Depending on the severity of the mutation and the

resulting defect, patients can present with a variety of signs and symptoms ranging from mild exercise intolerance and muscle weakness to neuromuscular disorders[32]. Additionally, mitochondrial myopathy can lead to whole-body metabolic impairments, such as weight gain, insulin resistance and type II diabetes.

ii. Introduction to skeletal muscle and insulin sensitivity

The primary role of insulin within the body is the maintenance of blood glucose homeostasis. When blood glucose levels rise, such as following a meal, insulin is secreted from the pancreatic β-cells and initiates glucose uptake in insulin-sensitive tissues (liver, adipose and skeletal muscle) by binding to the α-subunits of the plasma membrane insulin receptor[33]. This induces the tyrosine kinase activity of the intracellular β-subunit and leads to the tyrosine phosphorylation of the intracellular proteins insulin receptor substrates 1 and 2 (IRS1, IRS2), causing their activation[33]. Interaction between these proteins and phosphatidylinositol 3-kinase (PI3K) stimulates the translocation of glucose transporter GLUT4 vesicles from intracellular stores to the plasma membrane, allowing for glucose uptake into the cell[33]. While the precise mechanism between PI3K activation and GLUT4 translocation remains to be fully elucidated, it is hypothesized that it involves signaling through the proteins phosphatidylinositol (3,4,5)-triphosphate (PIP_3), 3-phosphoinositide-dependent protein kinase 1 (PDK), Akt, AS160 and protein kinase C (PKC)[33] (Fig. 4A).

Of the insulin-sensitive tissues, skeletal muscle is the largest and the primary site of glucose uptake[34]. It has been shown that skeletal muscle is responsible for up to 80% of whole-body glucose clearance following a glucose infusion[35]. It is not surprising, then, that any disruptions to skeletal muscle insulin signaling will impact whole body insulin sensitivity, or the

amount of insulin needed to maintain blood glucose levels within the normal range. Conversely, insulin resistance (IR) refers to the decreased ability of the body to respond to insulin signaling. A greater amount of insulin must be secreted from the pancreas to generate the same response as in an insulin sensitive individual. Over time, the ability of the pancreas to maintain this high level of insulin secretion becomes diminished and blood glucose levels rise. This progression often results in the development of type II diabetes (T2D), a disease characterized by high blood glucose levels and IR, and for which skeletal muscle IR is thought to be the main contributor[36].

iii. Impaired mitochondrial function and type II diabetes/insulin resistance

The primary risk factor for the development of IR and T2D is obesity, often caused by the combination of a high fat diet (HFD), such as the modern 'Western diet', with decreased physical activity. However, mitochondrial dysfunction has recently been described as another possible contributor. It has been shown that the consumption of a HFD results in the accumulation of lipids and lipid metabolites, such as diacylglycerols (DAGs) and ceramides, within the muscle. It is hypothesized that the accumulation of these intramyocellular lipids (IMCLs) is due to their incomplete oxidation within the mitochondria as a result of mitochondrial defects[37]. Various studies have correlated DAGs and ceramides with insulin resistance, most likely due to their ability to activate PCK and initiate a serine kinase cascade leading to the serine phosphorylation of IRS1[38–41]. This results in IRS1 inactivation, as well as inhibition of tyrosine phosphorylation, which would induce activation[42]. The subsequent reduction in PI3K activity reduces GLUT4 membrane translocation and decreases insulin-stimulated glucose uptake[42]. Ceramides can also inhibit Akt directly, further exacerbating the reduction in GLUT4 translocation[43] (Fig. 4B).

Decreased mitochondrial capacity with insulin resistance has been shown in human studies, with decreases in both mitochondrial content and function. An ~40% reduction in mitochondrial density was detected in individuals with IR, while subjects with T2D experienced decreased mitochondrial area as well as decreased mitochondrial protein and mtDNA content[39,44,45]. Genetic analyses indicate a decrease in the expression of a variety of genes associated with the oxidative phosphorylation pathway in T2D[46,47]. Further, T2D subjects show a decrease in electron transport chain activity, independent of mitochondrial content[45]. Although it is still a matter of debate whether mitochondrial dysfunction is a consequence or cause of insulin resistance, it is clear that a relationship exists.

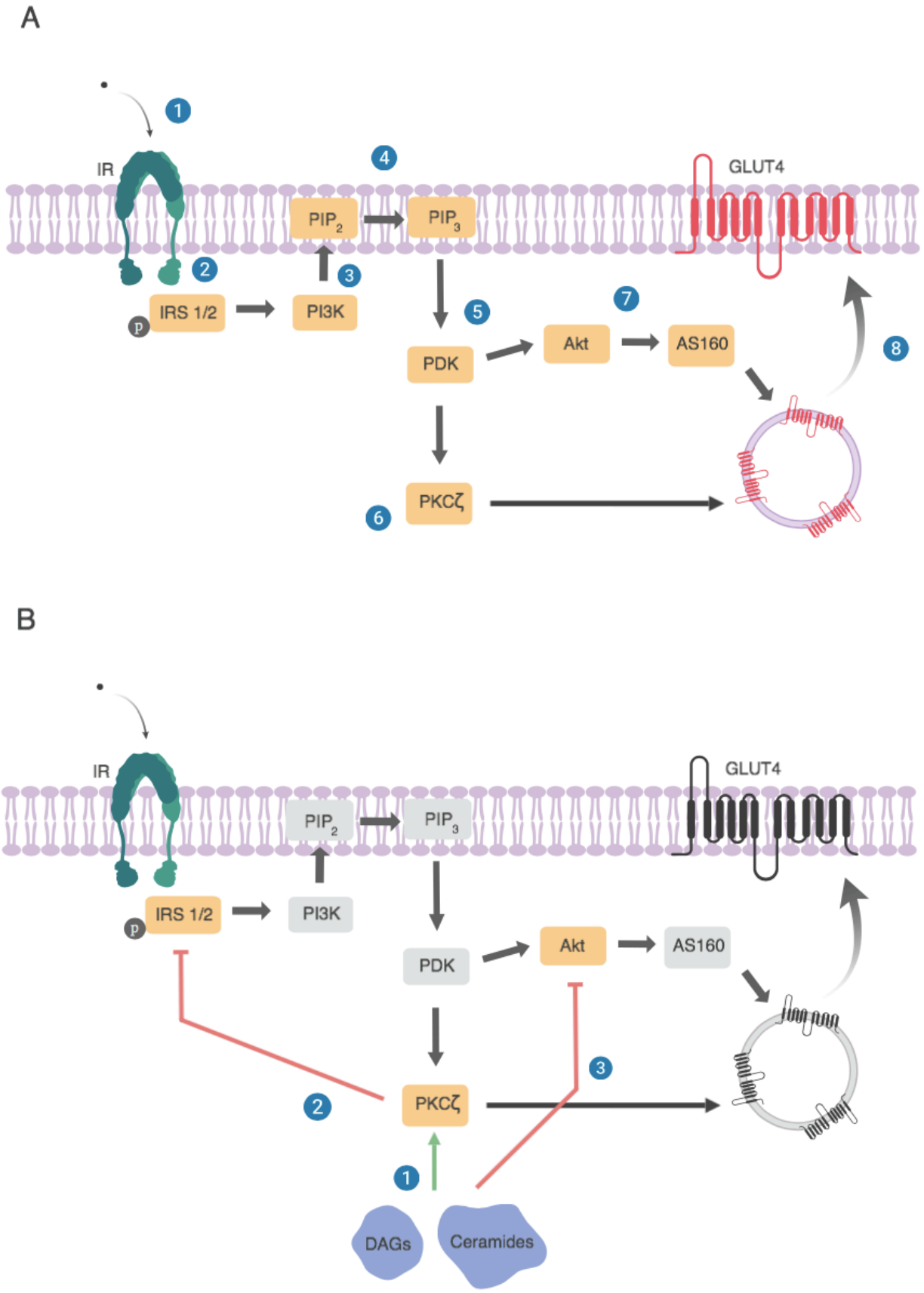
A
IR
GLUT4
PIP2
PIP3
IRS 1/2
PI3K
PDK
Akt
AS160
PKCζ
B
IR
GLUT4
PIP2
PIP3
IRS 1/2
PI3K
PDK
Akt
AS160
PKCζ
DAGs
Ceramides

Figure 4. Insulin signaling pathway and interference by lipid metabolites. Insulin signaling in skeletal muscle is initiated by insulin binding to the α-subunits of the plasma membrane insulin receptor (IR), inducing the tyrosine kinase activity of the intracellular β-subunit. Tyrosine phosphorylation activates insulin receptor substrate 1 and 2 (IRS1 and IRS2), allowing them to interact with phosphatidylinositol 3-kinase (PI3K). PI3K phosphorylates phosphatidylinositol (4,5)-bisphosphate (PIP_2) to phosphatidylinositol (3,4,5)-triphosphate (PIP_3) at the membrane, which acts through 3-phosphoinositide-dependent protein kinase 1 (PDK) and subsequently Akt, AS160 and protein kinase C (PKCζ) to cause GLUT4 translocation to the membrane and consequent glucose uptake into the cell (A). The accumulation of the lipid metabolites diacylglycerols (DAGs) and ceramides in the cell causes interference with the insulin signaling pathway. DAGs and ceramides can activate PKCζ, creating a serine kinase cascade leading to the serine phosphorylation, and inactivation, of IRS1 and IRS2. Ceramides are also able to inhibit Akt, further preventing GLUT4 membrane translocation (B).

iv. Mitochondrial structural and functional dependence on cytoskeletal proteins

It has long been known that the association between the mitochondria and the cytoskeleton is essential for mitochondrial localization and function[48]. Mitochondrial motility is reliant on microtubules, actin filaments and intermediate filaments, depending on the species and cell type[48]. However, the majority of research into the cytoskeleton and mitochondrial movement has been conducted in yeast cells and neurons, not skeletal muscle[49]. Yeast rely on the actin cytoskeleton for mitochondrial distribution and this connection appears to be dependent on the 'mitochore', a complex of proteins including Mmm1p, Mdm10p and Mdm12p, embedded within

the mitochondrial inner and outer membranes[50]. The loss of any one of these proteins results in impairments such as large, spherical mitochondria and mitochondrial delocalization[51–53]. It is interesting to note that the mitochore complex does not bind directly to actin but instead relies on an unidentified linker protein[54].

Within skeletal muscle, mitochondria seem to require a connection to intermediate filaments[55,56]. The striated muscle intermediate filament desmin is a scaffolding protein that links adjacent myofibrils at the z-disc and links the z-disc to the sarcolemma at the costamere[57]. However, it also appears to be important for mitochondrial localization[55,56]. In a desmin knockout mouse model, skeletal muscle mitochondria accumulate as clumps at the level of the subsarcolemma, while cardiac tissue displays extensive mitochondrial proliferation and swelling, degradation of the mitochondrial matrix and impairments to mitochondrial respiratory capacity[55]. Like the mitochore in yeast, it is predicted that desmin does not interact directly with the mitochondrial membrane but instead binds to an unknown, cross-linking protein[55].

3. Xin

a. Introduction to Xin

i. Original discovery of Xin

Xin is a striated muscle specific protein expressed in the cardiac and skeletal muscle of all vertebrates. Xin, which translates to heart in Chinese, was originally discovered while screening for novel genes regulating cardiac morphogenesis in chick embryos (previously known as cXin)[58], with subsequent analysis determining that cXin is also expressed in the developing somites[59]. A mammalian homologue found in mouse (previously known as mXin) confirmed the striated-muscle specific expression of Xin, as mXin mRNA was detected in the mouse

embryonic heart and somites, as well as in the adult heart and skeletal muscle, but not in other tissues[59]. Additionally, chick embryos incubated with cXin antisense oligonucleotides experienced abnormal cardiac morphogenesis and altered cardiac looping, emphasizing Xin's role in heart formation[59]. A human homologue for Xin has also been identified[60].

ii. Xin gene and protein information

Xin is coded for by the gene Xirp1, for Xin-repeat protein 1, previously known as Cmya1, for cardiomyopathy associated gene 1[61,62]. Xirp1 proteins contain a number of putative binding domains, including a nuclear localization signal, DNA binding domain and proline-rich regions, which suggest that Xin may act as a transcriptional regulator[59]. The presence of an Src homology 3 (SH3)-domain indicates the potential for a signaling role with other SH3-domain containing proteins[59]. Xin also contains unique 16-amino acid repeat (known as Xin repeat) regions, which have been shown to bind and organize actin microfilaments into networks[59]. Xirp1 contains two exons, with alternative splicing resulting in three protein isoforms: XinA (full length; 198kDa) XinB (carboxy-terminally truncated; 122kDa) and XinC (amino-terminally truncated; 56kDa)[63]. The amino-terminus of the Xin protein, present in the isoforms XinA and XinB, contains the proline-rich region capable of binding the EVH1 domain of the proteins Mena/VASP[63]. The carboxy-terminus, on the other hand, is present in isoforms XinA and XinC and binds to filamin C[63]. Mena/VASP is involved in the regulation of the actin cytoskeleton while filamin C is important in the attachment of the ends of myofibrils to the sarcolemma. There is evidence for the formation of a Mena/VASP-filamin C-xin complex bound to actin, suggesting that Xin plays a role in stabilization of the actin cytoskeleton[63]. Additionally, Xin binds to the protein Homer, important for calcium handling within skeletal muscle, as well as

aciculin, a protein closely associated with the actin cytoskeleton, and the thin-filament stabilizing protein nebulin[64–66]. Due to its assortment of binding partners, Xin is considered a multi-adaptor protein[65] (Fig. 5).

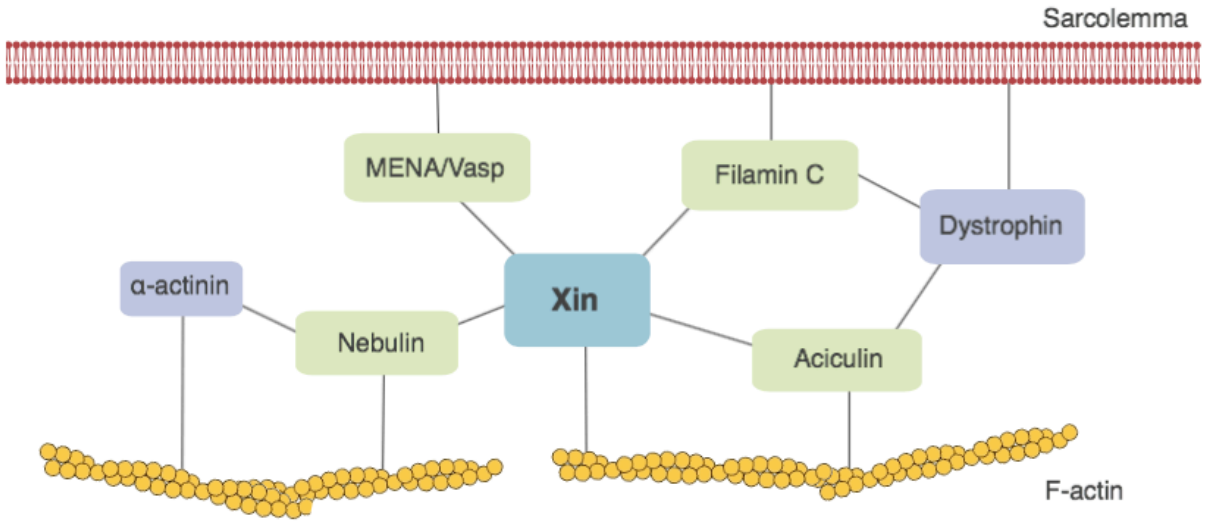

Figure 5. Xin and its cytoskeletal binding partners. Xin is a cytoskeletal multi-adaptor protein that binds with a number of other cytoskeletal proteins to form a network. Xin contains actin binding "Xin-repeats" that bind f-actin and organize these microfilaments into networks. Other Xin binding partners include MENA/Vasp and aciculin, both involved in the regulation of the actin cytoskeleton, filamin C, important for the attachment of the ends of myofibrils to the sarcolemma, and nebulin, a thin-filament stabilizing protein (direct Xin binding partners: green). Additionally, these proteins interact with a number of other cytoskeletal proteins, including α-actinin and dystrophin complex (indirect Xin binding partners: purple), making Xin a part of an even larger cytoskeletal protein network.

iii. Function of Xin

Within skeletal muscle, Xin was originally thought to be localized only to the myotendinous junction (MTJ), suggesting that Xin's only role was force conductance through this site[62]. However, previous studies from our lab have demonstrated Xin to be highly upregulated during the early stages of muscle regeneration in both rodents and humans[67,68]. Human skeletal muscle tissue with various degrees of myopathy displays an increase in Xin expression relative to the degree of muscle damage[67] while Xin expression in mice is increased and localized to active satellite cells and regenerating myofibres following cardiotoxin injury[68].

Studies conducted on Xin-/- mice, using a complete Xirp1 knockout model, XinABC-/- (Xin-/-), developed by Otten et al.[69], revealed a mild myopathic phenotype, characterized by a modest increase in centrally nucleated and necrotic fibres[70] but a very significant decrease in the regenerative capacity following muscle damage[70]. Xin-/- mice also display impaired skeletal muscle function, experiencing early fatigue during and decreased force-production following in-situ muscle stimulation[64]. While it was hypothesized that this decrease in force production may result from disrupted sarcomere structure, electron microscopy (EM) analysis instead revealed swollen and streaming mitochondria with abnormal cristae[64]. To determine the impact of these observed structural abnormalities on mitochondrial function, respiratory capacity was assessed using permeabilized muscle fibre bundles[64]. While no differences were initially detected in either complex I or complex II supported respiration, correcting to mitochondrial content indicated significant impairments in Xin-/- muscle at both sites, implying that individual mitochondria may be dysfunctional and that an increase in mitochondrial content appears to compensate for these deficiencies at the whole tissue level[64]. Finally, analysis of cellular fractions and skeletal

muscle using immunohistochemistry indicated that Xin is localized to both the mitochondria and the cytosol, suggesting that Xin has an effect, at least in part, on mitochondria directly.

4. References

1. Rassier, D. E. Sarcomere mechanics in striated muscles: from molecules to sarcomeres to cells. Am. J. Physiol.-Cell Physiol. **313,** C134–C145 (2017).

2. Gautel, M. & Djinović-Carugo, K. The sarcomeric cytoskeleton: from molecules to motion. J. Exp. Biol. **219,** 135–145 (2016).

3. Luther, P. K. The vertebrate muscle Z-disc: sarcomere anchor for structure and signalling. J. Muscle Res. Cell Motil. **30,** 171–185 (2009).

4. Henderson, C. A., Gomez, C. G., Novak, S. M., Mi-Mi, L. & Gregorio, C. C. Overview of the Muscle Cytoskeleton. in Comprehensive Physiology (ed. Terjung, R.) 891–944 (John Wiley & Sons, Inc., 2017).

5. Jaka, O., Casas-Fraile, L., López de Munain, A. & Sáenz, A. Costamere proteins and their involvement in myopathic processes. Expert Rev. Mol. Med. **17,** (2015).

6. Charvet, B., Ruggiero, F. & Le Guellec, D. The development of the myotendinous junction. A review. Muscles Ligaments Tendons J. **2,** 53–63 (2012).

7. Frontera, W. R. & Ochala, J. Skeletal Muscle: A Brief Review of Structure and Function. Calcif. Tissue Int. **96,** 183–195 (2015).

8. Hargreaves, M. Skeletal Muscle Metabolism During Exercise In Humans. Clin. Exp. Pharmacol. Physiol. **27,** 225–228 (2000).

9. Egan, B. & Zierath, J. R. Exercise Metabolism and the Molecular Regulation of Skeletal Muscle Adaptation. Cell Metab. **17,** 162–184 (2013).

10. Schönfeld, P. & Wojtczak, L. Short- and medium-chain fatty acids in energy metabolism: the cellular perspective. J. Lipid Res. **57,** 943–954 (2016).

11. Lundsgaard, A.-M., Fritzen, A. M. & Kiens, B. Molecular Regulation of Fatty Acid Oxidation in Skeletal Muscle during Aerobic Exercise. Trends Endocrinol. Metab. **29,** 18–30 (2018).

12. Takahashi, M. & Hood, D. A. Protein Import into Subsarcolemmal and Intermyofibrillar Skeletal Muscle Mitochondria. J. Biol. Chem. **271,** 27285–91 (1996).

13. Ferreira, R. et al. Subsarcolemmal and intermyofibrillar mitochondria proteome differences disclose functional specializations in skeletal muscle. PROTEOMICS **10,** 3142–3154 (2010).

14. Palmer, J. W., Tandler, B. & Hoppel, C. L. Biochemical differences between subsarcolemmal and interfibrillar mitochondria from rat cardiac muscle: effects of procedural manipulations. Arch. Biochem. Biophys. **236,** 691–702 (1985).

15. Koves, T. R. et al. Subsarcolemmal and intermyofibrillar mitochondria play distinct roles in regulating skeletal muscle fatty acid metabolism. Am. J. Physiol.-Cell Physiol. **288,** C1074–C1082 (2005).

16. Duchen, M. R. Mitochondria in health and disease: perspectives on a new mitochondrial biology. Mol. Aspects Med. **25,** 365–451 (2004).

17. Mitchell, P. & Moyle, J. Chemiosmotic Hypothesis of Oxidative Phosphorylation. Nature **213,** 137 (1967).

18. Bouillaud, F., Alves-Guerra, M.-C. & Ricquier, D. UCPs, at the interface between bioenergetics and metabolism. Biochim. Biophys. Acta BBA - Mol. Cell Res. **1863,** 2443–2456 (2016).

19. Zorov, D. B., Juhaszova, M. & Sollott, S. J. Mitochondrial Reactive Oxygen Species (ROS) and ROS-Induced ROS Release. Physiol. Rev. **94,** 909–950 (2014).

20. Guzy, R. D. & Schumacker, P. T. Oxygen sensing by mitochondria at complex III: the paradox of increased reactive oxygen species during hypoxia. Exp. Physiol. **91,** 807–819 (2006).

21. Elmore, S. Apoptosis: A Review of Programmed Cell Death. Toxicol. Pathol. **35,** 495–516 (2007).

22. Dunn, J. D., Alvarez, L. A., Zhang, X. & Soldati, T. Reactive oxygen species and mitochondria: A nexus of cellular homeostasis. Redox Biol. **6,** 472–485 (2015).

23. Oxenoid, K. et al. Architecture of the mitochondrial calcium uniporter. Nature **533,** 269 (2016).

24. Rizzuto, R., Stefani, D. D., Raffaello, A. & Mammucari, C. Mitochondria as sensors and regulators of calcium signalling. Nat. Rev. Mol. Cell Biol. **13,** 566 (2012).

25. Jornayvaz, F. R. & Shulman, G. I. Regulation of mitochondrial biogenesis. Essays Biochem. **47,** (2010).

26. Wu, Z. et al. Mechanisms Controlling Mitochondrial Biogenesis and Respiration through the Thermogenic Coactivator PGC-1. Cell **98,** 115–124 (1999).

27. Yoneda, M., Miyatake, T. & Attardi, G. Complementation of mutant and wild-type human mitochondrial DNAs coexisting since the mutation event and lack of complementation of DNAs introduced separately into a cell within distinct organelles. Mol. Cell. Biol. **14,** 2699–2712 (1994).

28. Youle, R. J. & van der Bliek, A. M. Mitochondrial Fission, Fusion, and Stress. Science **337,** 1062–1065 (2012).

29. Pagliuso, A., Cossart, P. & Stavru, F. The ever-growing complexity of the mitochondrial fission machinery. Cell. Mol. Life Sci. **75,** 355–374 (2018).

30. Twig, G. & Shirihai, O. S. The Interplay Between Mitochondrial Dynamics and Mitophagy. Antioxid. Redox Signal. **14,** 1939–1951 (2011).

31. Haas, R. H. et al. The In-Depth Evaluation of Suspected Mitochondrial Disease. Mol. Genet. Metab. **94,** 16–37 (2008).

32. Russell, A. P., Foletta, V. C., Snow, R. J. & Wadley, G. D. Skeletal muscle mitochondria: A major player in exercise, health and disease. Biochim. Biophys. Acta BBA - Gen. Subj. **1840,** 1276–1284 (2014).

33. Meo, S. D., Iossa, S. & Venditti, P. Skeletal muscle insulin resistance: role of mitochondria and other ROS sources. J. Endocrinol. **233,** R15–R42 (2017).

34. DeFronzo, R. A. et al. The Effect of Insulin on the Disposal of Intravenous Glucose: Results from Indirect Calorimetry and Hepatic and Femoral Venous Catheterization. Diabetes **30,** 1000–1007 (1981).

35. Thiebaud, D. et al. The effect of graded doses of insulin on total glucose uptake, glucose oxidation, and glucose storage in man. Diabetes **31,** 957–963 (1982).

36. DeFronzo, R. A. & Tripathy, D. Skeletal Muscle Insulin Resistance Is the Primary Defect in Type 2 Diabetes. Diabetes Care **32,** S157–S163 (2009).

37. Consitt, L. A., Bell, J. A. & Houmard, J. A. Intramuscular Lipid Metabolism, Insulin Action and Obesity. IUBMB Life **61,** 47–55 (2009).

38. He, J., Watkins, S. & Kelley, D. E. Skeletal Muscle Lipid Content and Oxidative Enzyme Activity in Relation to Muscle Fiber Type in Type 2 Diabetes and Obesity. Diabetes **50,** 817–823 (2001).

39. Morino, K. et al. Reduced mitochondrial density and increased IRS-1 serine phosphorylation in muscle of insulin-resistant offspring of type 2 diabetic parents. J. Clin. Invest. **115,** 3587–3593 (2005).

40. Petersen, K. F. et al. Mitochondrial dysfunction in the elderly: possible role in insulin resistance. Science **300,** 1140–1142 (2003).

41. Petersen, K. F., Dufour, S., Befroy, D., Garcia, R. & Shulman, G. I. Impaired mitochondrial activity in the insulin-resistant offspring of patients with type 2 diabetes. N. Engl. J. Med. **350,** 664–671 (2004).

42. Lowell, B. B. & Shulman, G. I. Mitochondrial Dysfunction and Type 2 Diabetes. Science **307,** 384–387 (2005).

43. Schubert, K. M., Scheid, M. P. & Duronio, V. Ceramide Inhibits Protein Kinase B/Akt by Promoting Dephosphorylation of Serine 473. J. Biol. Chem. **275,** 13330–13335 (2000).

44. Kelley, D. E., He, J., Menshikova, E. V. & Ritov, V. B. Dysfunction of mitochondria in human skeletal muscle in type 2 diabetes. Diabetes **51,** 2944–2950 (2002).

45. Ritov, V. B. et al. Deficiency of subsarcolemmal mitochondria in obesity and type 2 diabetes. Diabetes **54,** 8–14 (2005).

46. Mootha, V. K. et al. PGC-1alpha-responsive genes involved in oxidative phosphorylation are coordinately downregulated in human diabetes. Nat. Genet. **34,** 267–273 (2003).

47. Patti, M. E. et al. Coordinated reduction of genes of oxidative metabolism in humans with insulin resistance and diabetes: Potential role of PGC1 and NRF1. Proc. Natl. Acad. Sci. U. S. A. **100,** 8466–8471 (2003).

48. Anesti, V. & Scorrano, L. The relationship between mitochondrial shape and function and the cytoskeleton. Biochim. Biophys. Acta BBA - Bioenerg. **1757,** 692–699 (2006).

49. Wu, M., Kalyanasundaram, A. & Zhu, J. Structural and biomechanical basis of mitochondrial movement in eukaryotic cells. Int. J. Nanomedicine **8,** 4033–4042 (2013).

50. Boldogh, I. R. & Pon, L. A. Interactions of mitochondria with the actin cytoskeleton. Biochim. Biophys. Acta BBA - Mol. Cell Res. **1763,** 450–462 (2006).

51. Boldogh, I. R. et al. A protein complex containing Mdm10p, Mdm12p, and Mmm1p links mitochondrial membranes and DNA to the cytoskeleton-based segregation machinery. Mol. Biol. Cell **14,** 4618–4627 (2003).

52. Burgess, S. M., Delannoy, M. & Jensen, R. E. MMM1 encodes a mitochondrial outer membrane protein essential for establishing and maintaining the structure of yeast mitochondria. J. Cell Biol. **126,** 1375–1391 (1994).

53. Sogo, L. F. & Yaffe, M. P. Regulation of mitochondrial morphology and inheritance by Mdm10p, a protein of the mitochondrial outer membrane. J. Cell Biol. **126,** 1361–1373 (1994).

54. Boldogh, I., Vojtov, N., Karmon, S. & Pon, L. A. Interaction between Mitochondria and the Actin Cytoskeleton in Budding Yeast Requires Two Integral Mitochondrial Outer Membrane Proteins, Mmm1p and Mdm10p. J. Cell Biol. **141,** 1371–1381 (1998).

55. Milner, D. J., Mavroidis, M., Weisleder, N. & Capetanaki, Y. Desmin Cytoskeleton Linked to Muscle Mitochondrial Distribution and Respiratory Function. J. Cell Biol. **150,** 1283–1298 (2000).

56. Reipert, S. et al. Association of mitochondria with plectin and desmin intermediate filaments in striated muscle. Exp. Cell Res. **252,** 479–491 (1999).

57. Paulin, D. & Li, Z. Desmin: a major intermediate filament protein essential for the structural integrity and function of muscle. Exp. Cell Res. **301,** 1–7 (2004).

58. Wang, D. Z. et al. Differential displaying of mRNAs from the atrioventricular region of developing chicken hearts at stages 15 and 21. Front. Biosci. J. Virtual Libr. **1,** a1-15 (1996).

59. Wang, D. Z. et al. Requirement of a novel gene, Xin, in cardiac morphogenesis. Development **126,** 1281–1294 (1999).

60. Pacholsky, D. et al. Xin repeats define a novel actin-binding motif. J. Cell Sci. **117,** 5257–5268 (2004).

61. Gustafson-Wagner, E. A. et al. Loss of mXinα, an intercalated disk protein, results in cardiac hypertrophy and cardiomyopathy with conduction defects. Am. J. Physiol. Heart Circ. Physiol. **293,** H2680–H2692 (2007).

62. Feng, H.-Z. et al. Localization and function of Xinα in mouse skeletal muscle. Am. J. Physiol. - Cell Physiol. **304,** C1002–C1012 (2013).

63. van der Ven, P. F. M. et al. Unusual splicing events result in distinct Xin isoforms that associate differentially with filamin c and Mena/VASP. Exp. Cell Res. **312,** 2154–2167 (2006).

64. Al-Sajee, D. Investigating the roles of Xin in skeletal muscle and its satellite cell population. (2017).

65. Molt, S. et al. Aciculin interacts with filamin C and Xin and is essential for myofibril assembly, remodeling and maintenance. J Cell Sci **127,** 3578–3592 (2014).

66. Eulitz, S. et al. Identification of Xin-repeat proteins as novel ligands of the SH3 domains of nebulin and nebulette and analysis of their interaction during myofibril formation and remodeling. Mol. Biol. Cell **24,** 3215–3226 (2013).

67. Nilsson, M. I. et al. Xin Is a Marker of Skeletal Muscle Damage Severity in Myopathies. Am. J. Pathol. **183,** 1703–1709 (2013).

68. Hawke, T. J. et al. Xin, an actin binding protein, is expressed within muscle satellite cells and newly regenerated skeletal muscle fibers. Am. J. Physiol. Cell Physiol. **293,** C1636-1644 (2007).

69. Otten, J. et al. Complete loss of murine Xin results in a mild cardiac phenotype with altered distribution of intercalated discs. Cardiovasc. Res. **85,** 739–750 (2010).

70. Al-Sajee, D. et al. Xin-deficient mice display myopathy, impaired contractility, attenuated muscle repair and altered satellite cell functionality. Acta Physiol. Oxf. Engl. **214,** 248–260 (2015).

Xin as a novel regulator of mitochondrial morphology and bioenergetics in skeletal muscle

Molly A Gingrich[1], Dhuha Al-Sajee[1], Ananya Sharma[1], Cynthia M F Monaco[1], Athan G Dial[1], Grace Martin[1], Rimsha Chattha[1], Thomas J. Hawke[1]

[1]Dept of Pathology & Molecular Medicine, McMaster University

Abstract

Xin is a striated muscle specific, cytoskeletal adaptor protein that our lab has recently localized to the mitochondria and peri-mitochondrial regions of skeletal muscle. Further, we have identified mild mitochondrial structural and functional impairments in the skeletal muscle of Xin-/- mice. The objective of this study was to investigate the physiological effects of Xin deficiency in combination with the metabolic stress of a high fat diet, as well as the impact on skeletal muscle mitochondrial structure and function. Wild-type (WT) and Xin knockout (Xin-/-) mice were fed a high-fat diet (HFD- 60%kcal fat) for 8 weeks. HFD-fed Xin-/- mice did not gain greater body or fat mass relative to WT mice. However, Xin-/- mice had increased fasted blood glucose levels (Xin-/-: 15.8±1.042, WT: 10.7±0.652; $p<0.05$) and reduced glucose tolerance (AUC Xin-/-: 51.4±1.7, WT: 31.1±3.1; $p<0.05$) after 8 weeks of HFD feeding. Electron microscopy analysis revealed an ~1.5-fold (46.4%±7.5; $p<0.05$) increase in intermyofibrillar mitochondrial content and a ~2.8-fold (186.3%±9.6; $p<0.05$) increase in size, associated with mitochondrial swelling, streaming and loss of cristae. Complex I and complex II supported respiration were also impaired when corrected to mitochondrial content (complex I: JO_2 Xin-/-: 130.7±22.3, WT: 210.2±38.8; $p<0.05$; complex II: JO_2 Xin-/-: 124.4±13.9, WT: 175.6±20.9; $p<0.05$). We observed no changes to the protein content of either the autophagic proteins p62 or LC3, or the mitochondrial fission proteins Drp1 or Fis1 or fusion proteins Mfn1 or Mfn2. Overall, Xin-/- mice exhibited abnormal muscle mitochondrial morphology, decreased mitochondrial respiration and dysregulated glucose handling, independent of changes in body weight. Future studies are needed to identify Xin-specific binding partners and determine if Xin may be an unidentified contributor to mitochondrial myopathy and the development of metabolic disorders.

Introduction

Skeletal muscle is the largest organ in the human body and is principally responsible for both our physical and metabolic capacities. Accounting for up to 80% of whole-body glucose uptake[1,2] , skeletal muscle's high capacity for fuel usage is necessary to meet the metabolic demands of this tissue. The metabolic capacity of skeletal muscle is determined primarily by the mitochondrial population, which comprises approximately 4-7% of skeletal muscle volume[3,4]. Mitochondria are essential for energy production and use oxygen and fuel substrates to generate energy in the form of adenosine triphosphate (ATP) for muscle contraction, as well as other energy-dependent processes within the cell.

Any impairments to mitochondrial structure or function can cause disordered fuel handling and subsequently lead to the development of metabolic diseases such as obesity and type II diabetes[5]. Studies of skeletal muscle from type II diabetic individuals have repeatedly shown a downregulation of genes involved in mitochondrial metabolism, including those associated with the TCA cycle, oxidative phosphorylation and mitochondrial bioenergetics[6,7], as well as the decreased expression and activity of related proteins[8–10]. It has been proposed that mitochondrial dysfunction can lead to insulin resistance directly, with impairments to fat oxidation causing the accumulation of lipid metabolites and subsequent interference with the insulin signaling pathway[9]. Therefore, the maintenance of a healthy skeletal muscle mitochondrial pool is critical for the maintenance of whole-body metabolic function.

One factor that may be important for the preservation of skeletal muscle mitochondrial health is the striated muscle specific protein Xin. Our lab has recently localized Xin to the mitochondria

and peri-mitochondrial regions of skeletal muscle (Supp. Fig. 1)[11]. Preliminary data has identified the loss of Xin, in mouse skeletal muscle, to be associated with mitochondrial structural abnormalities and functional impairments, leading us to speculate that Xin plays an important role within this organelle[11]. Surprisingly, Xin knockout mice display a relatively normal phenotype in the unperturbed condition. In order to exacerbate the changes observed in Xin-/- mice on a chow diet and further elucidate a role for Xin within skeletal muscle mitochondria, we introduced the metabolic stress of a high fat diet to both WT and Xin-/- mice by feeding each group a 60%kcal fat, high fat diet (HFD) for 8 weeks. As a high fat diet (HFD) has been shown to cause an initial increase in mitochondrial function and as well as content[12], we were interested to see if Xin-/- mice were able to induce the same mitochondrial compensations. We hypothesized that the loss of Xin, in combination with the metabolic stress of a high fat diet, would result in metabolic dysfunction and mitochondrial impairments. Indeed, we identified that Xin-/- mice experience impaired blood glucose regulation, increased intramyocellular lipid content and mitochondrial structural and functional deficiencies.

Methods

Animals

All experiments conducted were approved by the McMaster University Animal Care Committee and were in accordance with the Canadian Council for Animal Care Guidelines. A total of 30 mice (n=30) were used throughout the study, with n values for each experiment provided within the figure legends. Xin-/- mice were developed as described by Otten et al. (2010). Male Xin-/- and C57BL6/J wild type (WT; Jackson Laboratories, Bar Harbor, ME, USA) mice were fed a standard chow diet [Envigo, Teklad #8640 Rodent Diet: energy (kcal/g) from protein (29%), fat

(17%), carbohydrate (54%)] until 8 weeks of age. At this time, mice were randomly assigned to either standard chow or high fat diet [TestDiet, 58126: energy (kcal/g) from protein (18.3%), fat (60.9%), carbohydrate (20.1%)] groups. All animals were housed under controlled conditions of 21°C, 50% humidity and 12 hour/12 hour light-dark cycle. Animals were provided enrichment materials and had ad libitum access to food and water. Fed state body mass was assessed weekly from 8 weeks of age to 16 weeks of age between 11:00 and 13:00 hours. Blood glucose via tail-nick was also assessed at this time (OneTouch Ultra glucometer; maximum 34mM; Johnson & Johnson).

Glucose tolerance test

Following 4 weeks and 8 weeks of HFD, WT and Xin-/- mice were fasted for 6 hours and blood glucose was assessed via tail-nick (OneTouch Ultra glucometer; maximum 34mM; Johnson & Johnson). An intraperitoneal glucose tolerance test (IPGTT) was performed following the 6 hour fast, with glucose injected IP (1g/kg body weight at 4 weeks; 0.5g/kg body weight at 8 weeks) and blood glucose assessed via tail-nick at 0, 20, 40, 60, 90 and 120 minutes.

Tissue collection

Animals were euthanized via cervical dislocation at 16 weeks of age. The tibialis anterior (TA), gastrocnemius plantaris (GP) and soleus (Sol) muscles were harvested and coated in optimal cutting temperature (O.C.T.) compound (Leica Biosystems, Richmond, IL) before freezing in liquid nitrogen cooled 2-methylbutane. TA muscle was also harvest for mitochondrial respiration (see below). The quadriceps muscles were flash frozen in liquid nitrogen. All samples were stored at -80°C until use.

Mitochondrial respiration

Permeabilized Muscle Fibres

Permeabilized muscle fibres were prepared as previously described[13]. Briefly, the red TA muscle was harvested from WT HFD and Xin-/- HFD mice. Muscle was immediately placed in ice-cold BIOPS buffer containing 50mM MES, 7.23mM K_2EGTA, 2.77mM CaK_2EGTA, 20mM imidazole, 0.5mM dithiothreitol (DTT), 20mM taurine, 5.77mM ATP, 15mM PCr, 6.56mM $MgCl_2 \cdot 6H_2O$ (pH 7.1). The muscle was then separated into several small muscle bundles and each bundle was gently separated along the longitudinal axis using needle-tipped forceps. Following this, bundles were treated with 40μg/mL saponin and 1μM CDNB in BIOPS buffer on a rotor at 4°C for 30 minutes to allow for permeabilization of the sarcolemma and depletion of glutathione as previously described[14]. Following incubation, fibres were washed in Buffer Z containing 105mM K-MES, 30mM KCl, 10mM KH_2PO_4, 5 $MgCl_2 \cdot 6H_2O$, 1mM EGTA, 5mg/mL BSA (pH 7.1) at 4°C.

Mitochondrial Respiration

The Oroboros O2k (Oroboros Instruments, Corp., Innsbruck, Austria) system was used to measure respiration in permeabilized muscle fibres at 37°C with constant stirring at 750rpm. Permeabilized fibres were added to 2mL of Buffer Z respiration medium containing 20mM creatine and chambers were hyperoxygenated to 350-375μM. State IV respiration was measured in the presence of 5mM pyruvate and 2mM malate. State III respiration was then measured by titrating 5mM ADP. Mitochondrial membrane integrity was next verified by adding 10μM Cytochrome c and samples with a >10% increase in respiration were excluded. For complex II specific respiration, complex I was inhibited with 0.5μM rotenone followed by 10mM succinate.

Histochemical staining and analysis

Oil Red O (ORO) staining was used to determine intramyocellular lipid (IMCL) content. TA muscle samples were sectioned at 10μm and incubated with ORO solution (Sigma, O0625) for 10 minutes. Following incubation, samples were washed under running water for 30 minutes. All imaging and analysis was conducted using a Nikon 90i microscope and Nikon NIS-Elements ND2 software (Melville, NY, USA). Muscle fibres were circled manually for subsequent analysis of lipid composition.

Electron microscopy imaging and analysis

Tibialis anterior muscles were collected from WT HFD and Xin-/- HFD mice for electron microscopy imaging and were fixed in 4% paraformaldehyde and 1.5% glutaraldehyde. Longitudinal sections were prepared on copper grids, contrasted with uranyl acetate and lead citrate and viewed in a JEOL JEM 1200 EX TEMSCAN transmission electron microscope (JEOL, Peabody, MA, USA) at McMaster University. Images were captured from non-overlapping sections at 10,000x and 30,000x magnification. 10,000x magnification images were subsequently analyzed using Nikon NIS-Elements ND2 software (Melville, NY, USA). Mitochondrial area, density and content were measured via manual circling of individual mitochondria and analyzed relative to total fibre area.

Western blot analysis

Western blots were completed using standard procedure with snap-frozen quadriceps muscle from WT and Xin-/- mice. Muscle was homogenized in lysis buffer and protein content was determined using a BCA assay. Lysates were run on 12% SDS-PAGE gel and transferred to PVDF membranes. Primary antibodies (p62 - 1:1000, Cell Signaling 8025; LC3 – 1:1000, Cell

Signaling 2775; DRP1 – 1:1000, Abcam 56788; FIS1 – 1:1000, Proteintech 10956-1-AP; MFN1 – 1:1000, Abcam 57602; MFN2 – 1:1000, Abcam 56889) were incubated overnight at 4°C. Appropriate horse radish conjugated secondary antibodies were applied (Abcam 6721; Abcam 6789). Chemiluminescent reagent (Biorad 1705061) was used to visualize proteins of interest.

Statistical analysis

All statistical analysis was conducted using GraphPad Prism 7.0. A Student's t-test or two-way ANOVA was used for comparison between groups and Bonferroni post-hoc analysis was performed. Statistical significance was set at a p value of less than 0.05. All data presented are mean ± SEM (standard error of the mean).

Results

No difference in weight gain or body composition between WT and Xin-/- mice in response to HFD

To determine the effects of the loss of Xin on whole-body metabolism, a HFD (60% kcal from fat) was administered to WT and Xin-/- mice for 8 weeks. No significant differences were seen in weight gain (measured weekly) at any time throughout the experimental period (Fig. 1A). Furthermore, no significant differences between groups were observed with respect to epididymal fat mass, tibialis anterior (TA) muscle and gastrocnemius-plantaris-soleus (GPS) muscle mass, either in absolute terms (data not shown) or when expressed as a percent of body weight (Fig. 1B-D).

Xin-/- HFD mice had increased fasted blood glucose levels and impaired glucose handling

Even in the absence of weight gain, metabolic impairments are often still present with consumption of a HFD and can precede changes to body composition. To assess impairments to glucose homeostasis, fasted blood glucose levels were measured in WT HFD and Xin-/- HFD mice following a 6 hour fast. Xin-/- mice had significantly higher fasted blood glucose levels than WT mice, with values considered clinically diabetic (>15mM) (Fig. 2A). A glucose tolerance test (GTT) was administered after 4 weeks of high-fat diet feeding and revealed significant impairments in the glucose handling abilities of Xin-/- HFD mice (Fig. 2B-C) with a trend ($p=0.07$) for significance when corrected to fasted blood glucose levels (Fig. 2D-E). After 8 weeks of high-fat feeding, the GTT was repeated, wherein Xin-/- mice experienced reduced glucose clearance compared to WT mice under both uncorrected (Fig. 2F-G) and corrected (Fig. 2H-I) conditions. Additionally, when corrected to fasted blood glucose, Xin-/- HFD mice had significantly greater blood glucose levels at 40, 60 and 90 minutes following the initiation of the GTT (Fig 2H).

Skeletal muscle of Xin-/- mice contained a greater number of lipid droplets and increased lipid droplet size

Impairments to glucose handling have been associated with an increase in intramyocellular lipid (IMCL) content and subsequent interference with the insulin signaling pathway[15]. To investigate the number of lipid droplets within WT HFD and Xin-/- HFD skeletal muscle, tibialis anterior muscle was analyzed using an Oil Red O stain, which stains for neutral lipids. Visual analysis revealed a relative homogeneous staining throughout the WT fibres. In contrast, Xin-/- fibres exhibited numerous, large droplets (Fig. 3A). Thresholding analysis confirmed a greater number

of lipid droplets and an increase in the size of these lipid droplets within Xin-/- HFD skeletal muscle (Fig. 3B).

Mitochondria within Xin-/- HFD skeletal muscle displayed morphological impairments and increased content

As mitochondria are primarily responsible for the generation of ATP from metabolic substrates, impairments to mitochondrial structure and/or function may account for increased presence of metabolic substrates (such as IMCL) within the muscle fibres. To determine if impairments to mitochondrial morphology were present, we analyzed TA muscle using electron microscopy. Intermyofibrillar mitochondria within WT HFD tissue showed limited abnormalities and primarily appeared as small, dark circles localized to either side of the z-disc (Fig. 4A-B). In contrast, mitochondria within Xin-/- HFD tissue displayed extensive swelling and streaming throughout the muscle fibres (Fig. 4C). Additionally, high magnification images suggested a disorganized cristae structure and the accumulation of debris within the mitochondrial matrix (Fig. 4D). Mitochondrial area was greater in Xin-/- HFD muscle compared to WT HFD (Fig. 4E), as was mitochondrial content (Fig. 4F). The resulting mitochondrial density, or the amount of fibre area occupied by mitochondria, was consequently increased within Xin-/- HFD muscle as well (Fig. 4G).

Mitochondria within Xin-/- HFD skeletal muscle displayed functional impairments

Due to the impairments to mitochondrial structure observed in Xin-/- HFD mice, we next aimed to determine if mitochondrial function was also impaired by performing high resolution respirometry in permeabilized TA muscle fibres. In absolute terms, no differences were observed

between WT HFD and Xin-/- HFD groups when maximal complex I respiration was stimulated through the addition of 5mM ADP (Fig. 5A). Similarly, no differences were observed in absolute terms when maximal complex II respiration was stimulated by the addition of 10mM succinate (Fig. 5B). Correction of the data using mitochondrial content, as measured by electron microscopy (EM), revealed significant deficiencies in both complex I (Fig. 5C) and complex II (Fig. 5D) supported respiration in Xin-/- HFD mice. This may indicate functional impairments to individual mitochondria, but no change at the whole tissue level, due to a compensatory increase in mitochondrial content.

Xin-/- HFD mice showed no dysregulation of autophagy

While an increase in mitochondrial content evidently results in no impairments to mitochondrial function at the whole tissue level and may act as a compensatory mechanism, we were interested to discern if the presence of these morphologically abnormal mitochondria were the result of alterations in autophagic proteins and, more specifically, whether autophagic proteins were significantly downregulated. In contrast to our hypothesis however, western blot analysis revealed no differences in the protein content of the autophagic protein p62 (Fig. 6A) and LC3 II/LC3 I protein ratio (Fig. 6B) between WT HFD and Xin-/- HFD mice.

Xin-/- HFD mice showed no dysregulation of mitochondrial fission or fusion

As our analyses were unable to detect any impairments to mitophagy in Xin-/- HFD mice, we next assessed if the observed increase in mitochondrial content could be a result of alterations in mitochondrial fission or fusion proteins. Western blot analysis of the protein content of the mitochondrial fission proteins Drp1 and Fis1 revealed no differences between Xin-/- HFD and

WT HFD mice (Fig. 7A-B). Similarly, there were no differences in the protein content of the mitochondrial fusion proteins Mfn1 or Mfn2 (Fig. 7C-D).

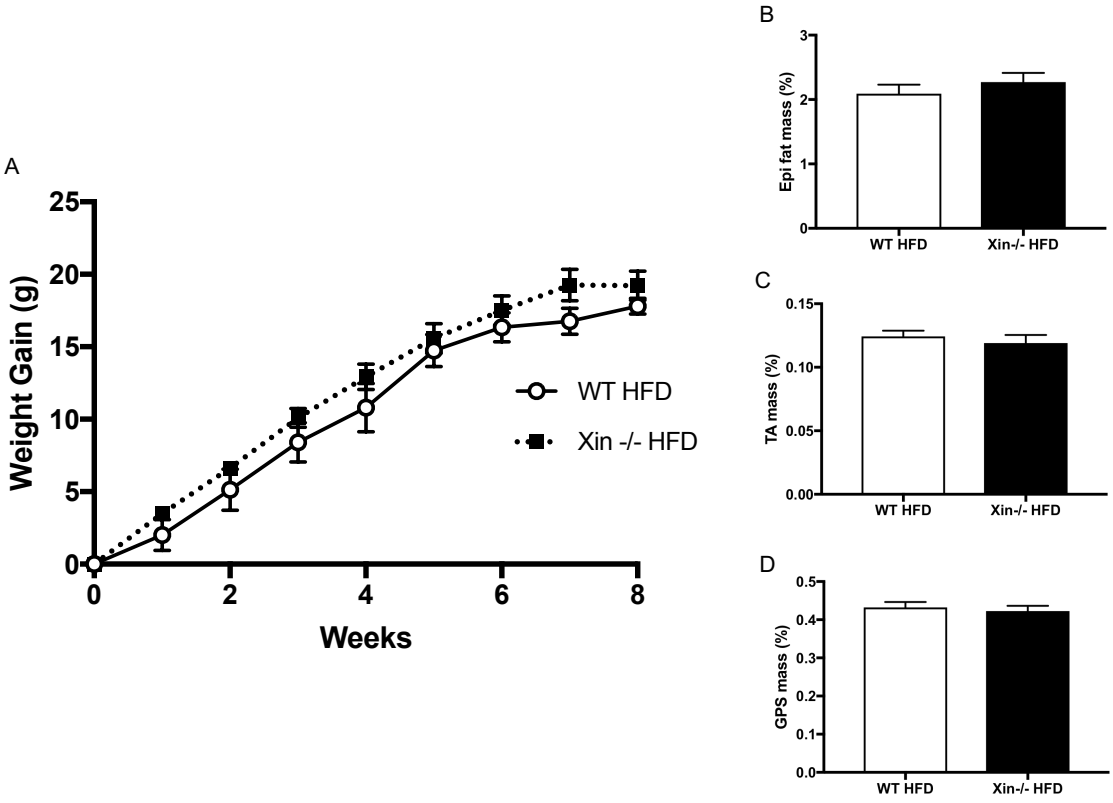

Figure 1. Xin-/- mice experienced no increase in weight gain or change in body composition compared to WT mice when fed a HFD. A) Body weight measurements over 8 weeks of HFD feeding in Xin-/- and WT mice revealed no significant differences in weight gain between the two groups. Epididymal fat, as well as TA and GPS muscles, were weighed at harvest and percent of body composition was determined. No significant differences were seen between WT and Xin-/- mice in any tissue, indicating no change to body composition (B-D). Values represent mean ± SEM. *P < 0.05. N=6/group.

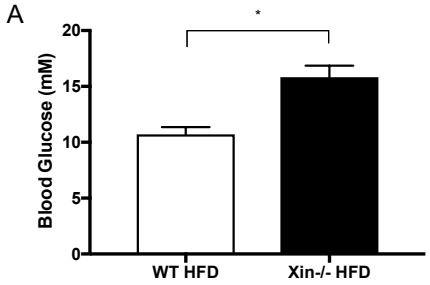
A
Blood Glucose (mM)
20
15
10
5
0
*
WT HFD
Xin-/- HFD

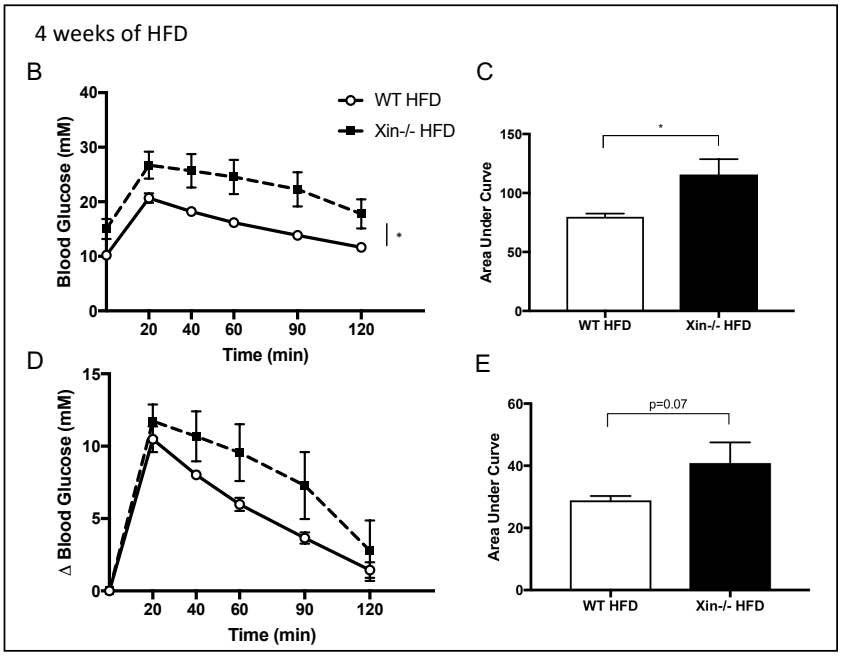
4 weeks of HFD
B
WT HFD
Xin-/- HFD
Blood Glucose (mM)
40
30
20
10
0
20 40 60 90 120
Time (min)
*
C
Area Under Curve
150
100
50
0
*
WT HFD
Xin-/- HFD
D
Δ Blood Glucose (mM)
15
10
5
0
20 40 60 90 120
Time (min)
E
Area Under Curve
60
40
20
0
p=0.07
WT HFD
Xin-/- HFD

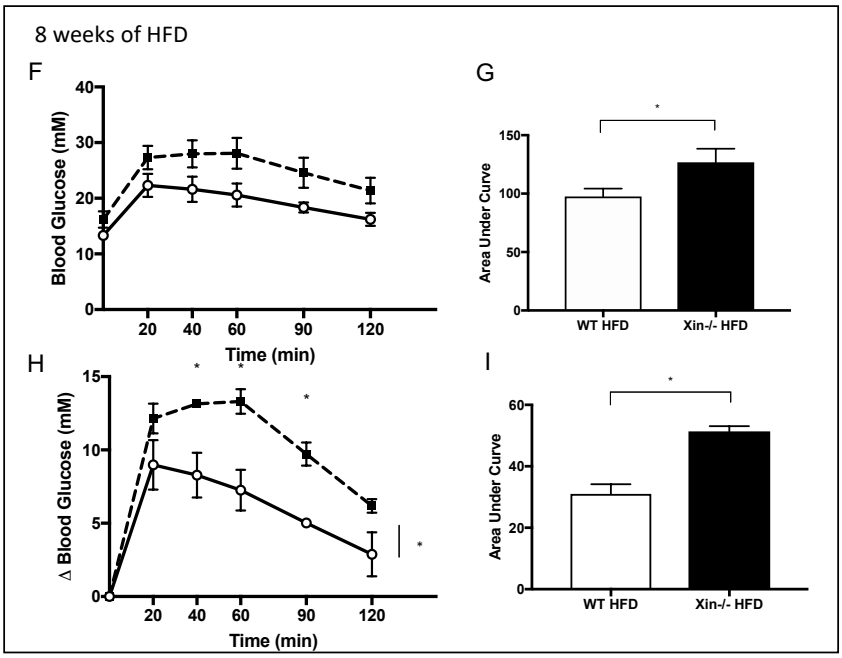
8 weeks of HFD
F
Blood Glucose (mM)
40
30
20
10
0
20 40 60 90 120
Time (min)
G
Area Under Curve
150
100
50
0
*
WT HFD
Xin-/- HFD
H
Δ Blood Glucose (mM)
15
10
5
0
* * *
*
20 40 60 90 120
Time (min)
I
Area Under Curve
60
40
20
0
*
WT HFD
Xin-/- HFD

Figure 2. Xin-/- mice experienced increased fasted blood glucose levels after 8 weeks of HFD and impaired glucose handling after 4 and 8 weeks of HFD.

(A) Blood glucose levels were significantly higher in Xin-/- HFD mice compared to WT HFD mice following a 6 hour fast and were within the range indicative of diabetes (>15mM). Following an 1mg/g intraperitoneal glucose injection after 4 weeks of HFD, Xin-/- mice displayed significant impairments in their glucose handling abilities (B-C), however not when corrected to fasted blood glucose ($p=0.07$; D-E). Following a 0.5mg/g intraperitoneal glucose injection after 8 weeks, Xin-/- mice displayed significant impairments under both uncorrected (F-G) and corrected (H-I) conditions. Values represent mean ± SEM. *$P < 0.05$. N=5-12/group.

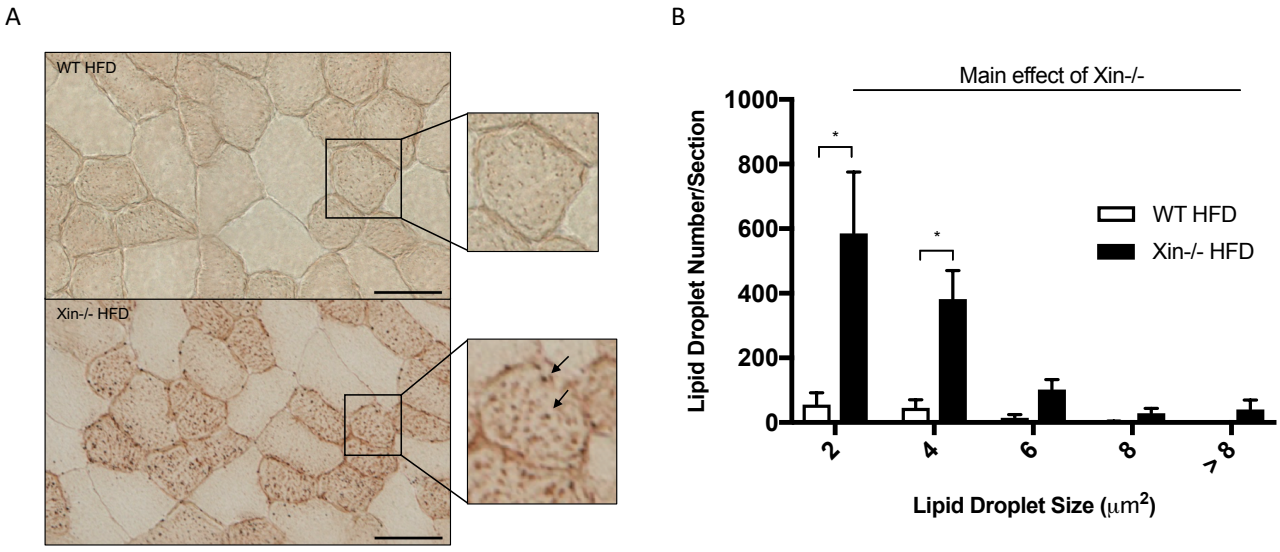

Figure 3. Xin-/- HFD mice had an increase in lipid droplet number and size in skeletal muscle compared to WT HFD mice. A) Representative images from WT and Xin-/- TA muscle showed a homogenous staining pattern in WT, but the appearance of larger lipid droplets within Xin-/- skeletal muscle. Scale bar = 50μm. B) Thresholding analysis confirmed that Xin-/- skeletal muscle contained a greater number of larger lipid droplets when compared to WT fibres. Values represent mean ± SEM. *P < 0.05. N=5/group; 150 fibres/animal.

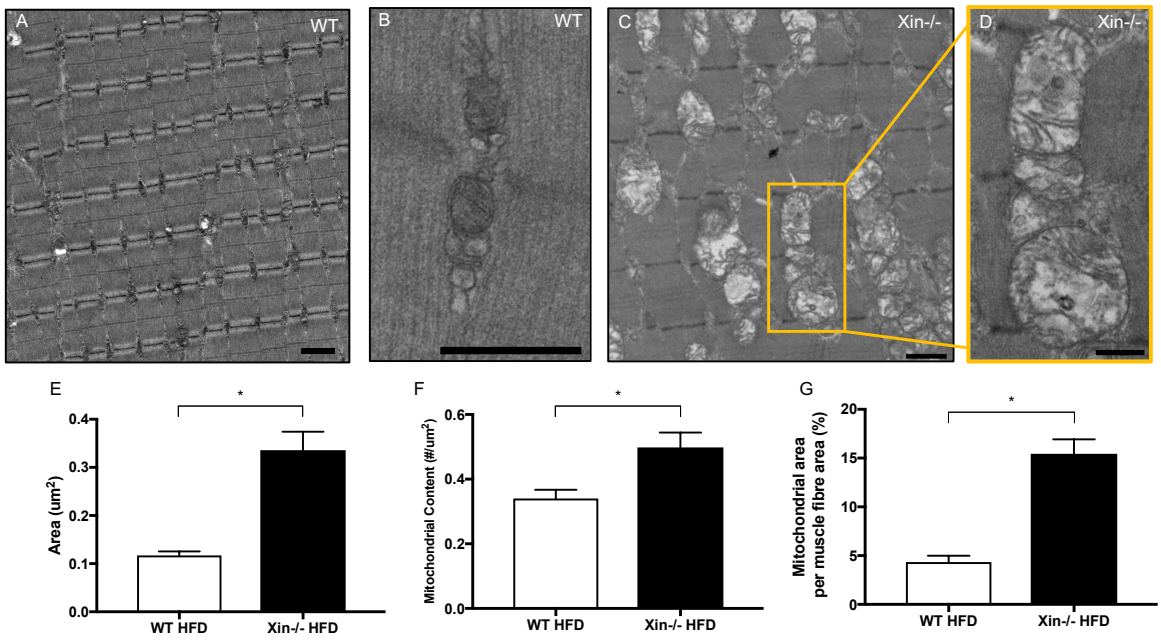

Figure 4. Xin-/- skeletal muscle contained mitochondria with an abnormal morphology, increased area, content and density. WT mitochondria appeared primarily as small, dark circles localized to either side of the z-disc, with mild mitochondrial swelling presumably as a result of HFD (A-B), while Xin-/- mitochondria displayed extensive swelling and streaming throughout the muscle tissue (C). Xin-/- mitochondria contained abnormal cristae and had an accumulation of debris within the mitochondrial matrix (D). Analysis of intermyofibrillar (IMF) mitochondria using electron microscopy indicated an increased mitochondrial area in Xin-/- tibialis anterior muscle (E). Mitochondrial content was also increased (F), as was the percent of fibre area composed of mitochondria (i.e. density) (G). (A, C) Scale bar=1μm; (C) Scale bar=500nm. Values represent mean ± SEM. *$P < 0.05$. N=2-3/group with 3-7 replicates/sample.

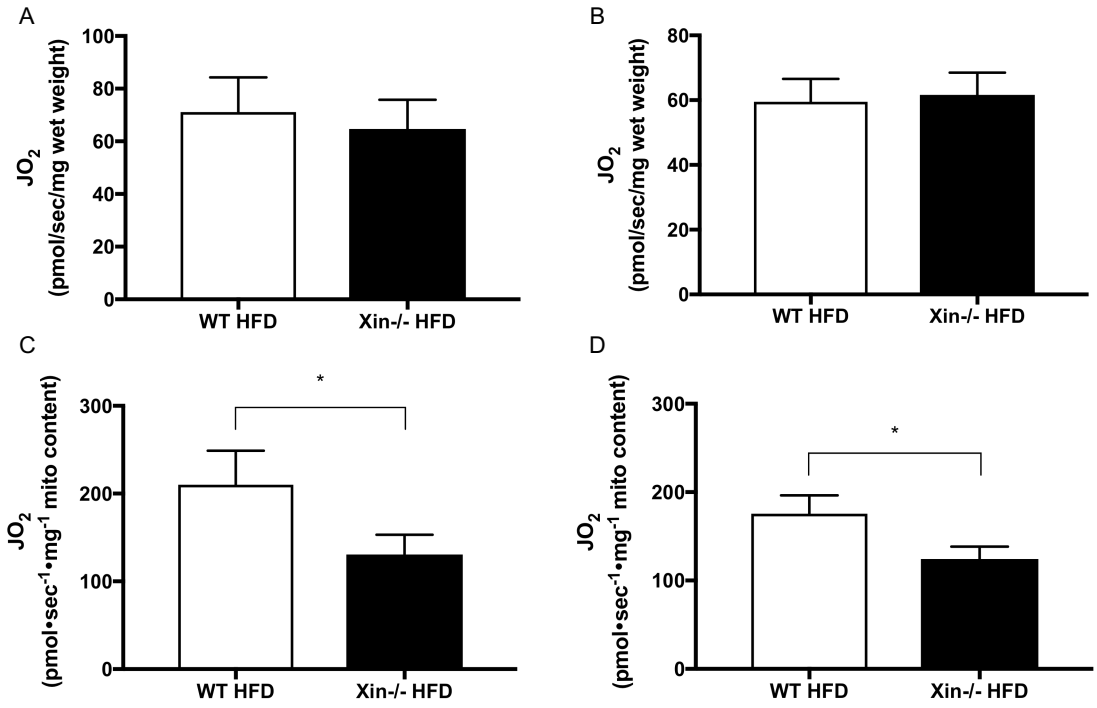

Figure 5. Xin-/- HFD skeletal muscle mitochondria experienced deficiencies in complex I and complex II supported respiration when corrected to mitochondrial content. Xin-/- and WT mice displayed no difference in complex I supported (A) or complex II supported (B) respiratory capacity when measured using permeabilized muscle fibres from TA muscle. However, when corrected to mitochondrial content, Xin-/- mice displayed significant impairments in both complex I (C) and complex II (D) supported respiration. Values represent mean ± SEM. *P < 0.05. N=4-6/group.

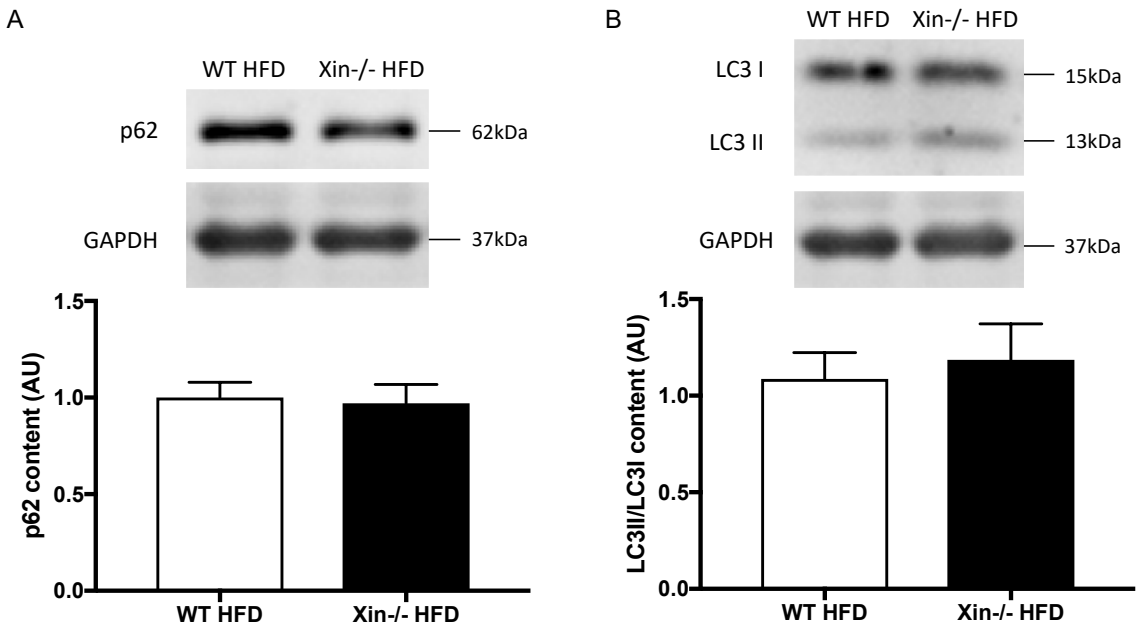

Figure 6. Xin-/- HFD and WT HFD mice experienced no difference in autophagic protein content. Analysis of western blots for p62 and LC3 II/LC3 I revealed no differences in the content of either protein in the skeletal muscle of Xin-/- HFD and WT HFD mice (A-B). Values represent mean ± SEM. *P < 0.05. N=9-12/group.

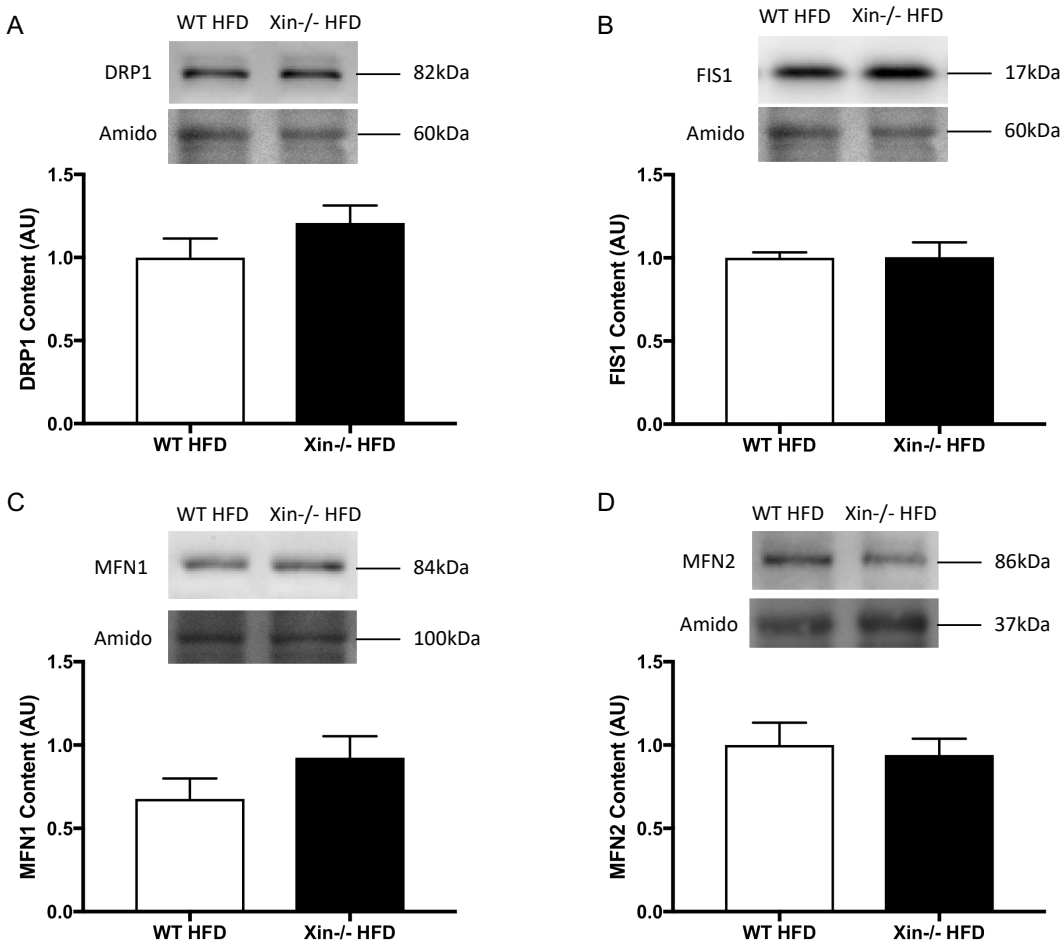

Figure 7. Xin-/- HFD and WT HFD mice experienced no difference in mitochondrial fission or fusion protein content. Analysis of western blots for the mitochondrial fission proteins DRP1 and FIS1 revealed no differences in the content of either protein in the skeletal muscle of Xin-/- HFD and WT HFD mice (A-B). There was also no difference in the protein content of the mitochondrial fusion proteins MFN1 or MFN2 (C-D). Values represent mean ± SEM. *P < 0.05. N=10-12/group.

Discussion

The aim of the current study was to determine the effects of loss of Xin on skeletal muscle mitochondrial morphology and bioenergetics, as well as on whole body metabolism, in a Xin-/- mouse model. When combined with diet induced obesity, loss of Xin resulted in deficiencies in blood glucose regulation, an increase in intramyocellular lipid content and impairments to mitochondrial structure and function.

Loss of Xin led to a diabetic phenotype in mice fed a HFD

Our lab has previously shown Xin to be localized to skeletal muscle mitochondria or the perimitochondrial area and demonstrated that the loss of Xin resulted in mild impairments to mitochondrial structure and function[11]. Here, we observed that the administration of a high fat diet in Xin-/- mice exacerbated these mitochondrial deficiencies and additionally compromised blood glucose regulation.

Interestingly, metabolic changes occurred independent of weight gain, as no differences in either weight gain or body composition were identified between Xin-/- and WT mice in response to HFD. However, an increase in fasted blood glucose levels of Xin-/- mice to ~16mM was particularly interesting, as this exceeds the threshold in which both mice and humans are considered to be diabetic[16]. Impairments to blood glucose clearance were also observed in Xin-/- mice and further contributed to the diabetic phenotype.

Mitochondrial structural and functional impairments occurred with loss of Xin and may explain the diabetic phenotype

To determine the mechanism behind increased fasted blood glucose levels and impaired glucose handling in Xin-/- mice, we next assessed intramyocellular lipid (IMCL) content. IMCLs are ectopic fat stores within muscle, often due to impaired mitochondrial fat oxidation, and are primarily made up of inert triacylglycerols (TAGs)[17,18]. However, a smaller percentage of IMCLs are made up of active lipid metabolites such as diacylglycerols (DAGs) and ceramides. These intermediates also increase with IMCL synthesis and degradation and can interfere with the insulin signaling pathway to inhibit glucose uptake[8]. IMCL content has been shown to increase by 25-50% in humans with obesity and diabetes when compared to lean non-diabetic controls[8]. Interestingly, increases of 60-80% have also been observed in the muscle of lean, insulin-resistant offspring of parents with T2D[19,20]. The presence of increased IMCL content concurrent with insulin resistance is consistent with our observations in Xin-/- animals.

As previously noted, mitochondrial impairments are often a primary cause of increased IMCL content. Under physiological conditions, fatty acids are broken down into acetyl-CoA within the mitochondrial matrix. However, dysfunctional mitochondria are unable to complete this process and incompletely oxidized lipids can build up within the cell[21]. To determine if mitochondrial dysfunction may have been the cause of increased IMCL content in Xin-/- mice, we assessed mitochondrial structure using electron microscopy. Xin-/- fibres had significantly greater mitochondrial swelling and streaming compared to WT fibres, as well as abnormal cristae and an accumulation of debris within the mitochondrial matrix. We also noted that Xin-/- fibres experienced an increase in mitochondrial content and we predicted that this may be a compensatory mechanism for impaired mitochondrial function - a hypothesis that was supported by our assessments of mitochondrial respiratory capacity. No differences were seen in

respiratory capacity between Xin-/- and WT mice using permeabilized muscle fibres but defects were detected in Xin-/- mice when respiratory values were corrected to mitochondrial content. This led us to believe that Xin-/- mice experienced functional deficiencies at the individual mitochondrial level and that an increase in mitochondrial content acted to maintain function at the level of the whole tissue.

Loss of Xin did not impact the protein content of autophagic or mitochondrial fission/fusion proteins

Alternatively, increased mitochondrial content in Xin-/- mice may be explained by a decrease in mitophagy, or the selective degradation of damaged mitochondria. However, when the content of the autophagic proteins p62 and LC3 were analyzed, no differences between Xin-/- and WT mice were observed, implying that mitophagy was not impaired. While LC3 is generally considered to be a good marker of autophagosome content, the lipidated form of LC3, LC3-II, has also been found ectopically, where its production is autophagy-independent[22]. Therefore, autophagy may be suppressed even in the presence of LC3, making autophagy defects undetectable by western blot. Another limitation of our analysis is that autophagic flux was not assessed. Autophagy is a dynamic process that is difficult to characterize using static measures and, instead, inhibitors of various stages of autophagy are often used to determine if autophagy initiation or downstream processes are impaired. Our western blot analysis may not have captured these differences, providing an interesting area for future investigation.

We predicted that in the absence of decreased mitophagy, an increase in mitochondrial fission would be observed to account for the increased mitochondrial content. Surprisingly, there were

no differences in the protein content of the fission proteins Drp1 and Fis1 or fusion proteins Mfn1 and Mfn2 between Xin-/- and WT mice, indicating no differences in mitochondrial fission or fusion between the two groups. One explanation may be that processes independent of fission and fusion protein content may have been responsible for altered mitochondrial dynamics. For example, F-actin interactions with mitochondria are necessary to promote mitochondrial fission and inhibit fusion[23]. Xin's ability to bind to F-actin[24] could make it an unknown player in this process, with the loss of Xin altering these interactions and impacting mitochondrial dynamics. Alternatively, mitophagy may have been impaired in Xin-/- mice, but our analysis of autophagic protein content may have been unable to detect this deficiency, as explained above.

Xin may function as a mitochondrial tether to maintain mitochondrial function

We have shown that the loss of Xin resulted in significant mitochondrial structural and functional deficiencies resulting in metabolic disease, but the mechanism underlying these changes remains elusive. One potential explanation may be that Xin acts as a tether, binding mitochondria to the cytoskeleton or to adjacent organelles. There is currently limited data regarding the identities of proteins involved in anchoring mitochondria within the cell, however significant impairments occur upon mitochondrial delocalization, with striking similarities to those observed in Xin-/- mice (see below).

Mitochondrial associated ER membranes (MAMs)

One site of mitochondrial contact that has gained increasing attention in recent years is the mitochondrial associated ER membrane (MAM), required for close contact between mitochondria and the endoplasmic/sarcoplasmic reticulum (ER/SR). These sites are important

for many processes including calcium transport, autophagy and mitochondrial dynamics and the loss of MAM integrity can consequently lead to impairments to all of these processes. Additionally, MAM dysfunction has been associated with deficiencies in glucose regulation, as liver specific knockout mice of known MAM proteins including Mfn2 or mTORC2 display metabolic impairments characterized by hyperglycemia and glucose intolerance[25,26] . Interestingly, many of the proteins involved in tethering mitochondria to the SR have yet to be characterized[27]. While Xin's partial co-localization to the mitochondrial and peri-mitochondrial areas initially led us to consider a role for Xin as a tether at MAMs, the phenotypic similarities between Xin-/- mice and various models of MAM dysregulation further supported our hypothesis.

MAM dysregulation and loss of Xin both result in mitochondrial swelling, possibly through changes to calcium signaling

Various studies have identified calcium uptake as a contributing factor to mitochondrial swelling, driven primarily by the subsequent loss of inner membrane permeability and changes to osmotic gradients[28]. A greater number of connections between the ER and mitochondria, also known as an increase in MAM content, has been shown to result in increased mitochondrial calcium uptake[29]. Swelling of mitochondria within the liver has been observed in both genetic and high fat diet mouse models of obesity, with an enrichment in MAMs and the subsequent increase in calcium flux shown to be the mechanism behind these changes[30]. These findings may be consistent with our observations in the skeletal muscle of Xin-/- mice, where we observed mitochondrial swelling. Although neither calcium flux nor MAM content was analyzed, this may be an interesting area for future research.

MAM dysregulation and loss of Xin may both result in impaired mitophagy

In 2013, Hamasaki et al. identified MAMs as the site of autophagosome formation, as the early-autophagosome markers ATG14 and ATG5 were found localized exclusively to these sites following starvation-induced autophagy[31]. Disruption of MAM integrity was shown to significantly inhibit autophagosome formation[31]. MAMs also play a role in mitophagy, or mitochondrial-specific autophagy. The mitophagy-related proteins PINK1 and BECN1 translocate to MAMs following mitophagic stimuli to initiate the formation of autophagosome precursors[32]. MAM integrity is most likely essential for this process as well, although the impact of MAM dysregulation on autophagosome formation in the presence of mitophagic stimuli has yet to be established. In either case, impaired autophagosome formation inhibits the removal of dysfunctional mitochondria, leading to the accumulation of damaged organelles throughout the cell. In the current study, Xin-/- mice experienced an accumulation of swollen, dysfunctional mitochondria within skeletal muscle. While we detected no differences in the content of the autophagic proteins p62 and LC3 when compared to WT mice, it is still possible that the loss of Xin led to MAM dysregulation and subsequent impairments to autophagosome formation. A block in the initial stages of autophagy may not affect the content of autophagic proteins associated with later autophagic stages such as p62 and LC3. In one study, the early-stage autophagy inhibitor verteporfin was shown to inhibit autophagosome formation without affecting LC3-II content[33]. Still, the connections between loss of Xin, impaired autophagy and MAM dysregulation remain primarily speculative and require further investigation.

MAM dysregulation and loss of Xin may both result in impaired mitochondrial dynamics

Research has indicated that mitochondrial fission and fusion are also highly dependent on MAMs[34,35]. Contacts between the ER and mitochondria mark sites of future mitochondrial fission, with up to 94% of division events occurring at MAMs and the fission protein Drp1 localizing to this region[36]. The mitochondrial fusion protein Mfn2 functions as a tether at MAMs, connecting the SR and mitochondria, and the loss of Mfn2 was shown to increase the distance between these two organelles in cells[37]. Mfn2 deficiency has also been associated with obesity and T2D. Liver-specific Mfn2-/- mice experience impaired insulin signaling in liver and skeletal muscle[25] while individuals with obesity and T2D have a reduction in skeletal muscle Mfn2 protein content[38]. No differences in the content of fission and fusion proteins were observed between Xin-/- and WT mice, but MAM dysregulation may have occurred. Drp1 protein content and MAM integrity are not necessarily related, as depletion of Drp1 can prevent mitochondrial fission but does not affect MAMs and MAM dysregulation can alter fission but has an unknown effect on Drp1 protein content[36]. Loss of Xin could also result in MAM dysregulation independent of Mfn2 content, as the effect of the loss of MAM tethers on the content of other proteins has not been investigated.

MAM dysregulation and loss of Xin both result in impaired glucose homeostasis

Finally, MAMs are involved in the regulation of glucose homeostasis, potentially via both direct and indirect methods. A recent study by Tubbs et al. associated MAM disruption with palmitate-induced insulin resistance in human myotubes and, strikingly, found that an experimental increase in MAM content restored insulin signaling[39]. Myotubes from obese and T2D human subjects had reduced MAM content that was positively correlated to impairments in the insulin

signaling pathway[39]. While the mechanism behind these changes is still under investigation, MAM disruption was found to precede mitochondrial dysfunction and insulin resistance in both genetic and diet-induced mouse models of obesity and T2D[39]. Reduced calcium transfer between the ER and mitochondria supports organelle miscommunication as a mechanism behind the development of insulin resistance, while MAM disruption can alter mitochondrial structure and function leading to impaired lipid oxidation, IMCL accumulation and interference with the insulin signaling pathway as described above[39].

Recent studies have theorized that a more direct connection between MAM disruption and insulin resistance is also possible, as a number of key insulin signaling proteins including Akt, mTORC2 and PTEN are localized to MAMs[26,40,41]. Further, MAM disruption can occur as a result of high glucose levels resulting in mitochondrial fission and impaired respiration[42]. Regardless of the whether a direct or indirect mechanism is primarily responsible for the link between MAM disruption and insulin resistance, it appears that the connection between the SR and mitochondria is vital for the preservation of metabolic health. While the function of Xin as a MAM tether remains hypothetical, both the mitochondrial and metabolic impairments resulting from MAM dysfunction and their similarities to those seen in Xin-/- mice make this an intriguing area for future investigation.

Desmin

Similar to Xin's potential role as a tether at MAMs, Xin may act to connect mitochondria to the cytoskeleton. Mitochondria are dependent on cytoskeletal connections, in addition to their

associations with the SR, for proper localization and function within skeletal muscle[43]. However, as with MAMs, the proteins mediating these connections are largely unknown[43].

In striated muscle, an association between mitochondria and the intermediate filament protein desmin appears to be critical in maintaining mitochondrial structure and function. Desmin, like Xin, is a muscle-specific protein that forms a part of the complex network required for the maintenance of muscle structure[44]. In addition to linking adjacent myofibrils at the z-disc and providing a connection between the sarcomere and the sarcolemma at costameres, desmin filaments have been purported to extend from the z-disc and associate with mitochondria[45,46]. The importance of this connection is highlighted by experiments conducted in desmin knockout mice, where the loss of desmin resulted in significant mitochondrial proliferation, swelling and matrix degradation (Supp. Fig. 2A). While this work was conducted primarily in cardiac muscle, there are noticeable similarities to the changes seen in Xin-/- skeletal muscle (Supp. Fig. 2B). In both instances, the mitochondrial population has been expanded both in size and, with severe swelling leading to abnormal cristae structure. These structural impairments appear to lead to functional deficiencies as well, as mitochondrial respiration, assessed using permeabilized fibres bundles, indicated a significant reduction in the maximal rate of ADP-stimulated oxygen consumption in both the cardiac and soleus muscle of desmin-/- mice and resembled observations in Xin-/- skeletal muscle[47].

In spite of the significant mitochondrial abnormalities that occur with the loss of desmin, it is predicted that mitochondria do not interact with desmin directly[47]. Instead, the connection is thought to be mediated by an unidentified linker protein[47]. One study proposed that this linker

protein may be plectin, a protein found primarily at the z-disc and a known binding partner of desmin, however there has been little functional data to support this claim[48,49]. Instead, the phenotypic similarities between desmin-/- and Xin-/- mice led us to consider Xin as an additional part of the desmin-mitochondrion complex or as the linker protein itself.

Additional information has provided support to this theory. As previously noted, Xin has been localized to both the mitochondrial and peri-mitochondrial regions of skeletal muscle and some evidence suggests that it may be located at the z-disc as well[11]. These findings reveal a distribution pattern for Xin that is remarkably similar to that of desmin. To further investigate this, we performed immunohistochemistry on skeletal muscle tissue and identified a Pearson's correlation co-efficient of 0.72 between Xin and desmin (Supp. Fig. 3), again suggesting that these proteins may colocalize. Further, Xin and desmin contain proline-rich regions that have been shown to bind SH3 domains[50,51]. Both may interact with the actin-binding protein nebulin, which is thought to act as a ruler to regulate thin filament length during sarcomere assembly, although the interaction between desmin and nebulin in vivo has not been fully resolved[51–53] . Whether Xin is able to interact with desmin directly remains to be determined, however this information has provided interesting preliminary evidence.

Given Xin's characterization as a cytoskeletal adaptor protein, it may be likely that Xin functions as a tether between mitochondria and the cytoskeleton instead of between the mitochondria and the SR. The consequences of the loss of mitochondrial connections with the cytoskeleton in skeletal muscle have not been extensively studied, with little research apart from the previously described study in desmin-/- mice. Presumably, the resultant mitochondrial delocalization would

cause many of the same deficiencies associated with disrupted MAMs, including impaired mitophagy, mitochondrial dynamics and glucose homeostasis, as many of these impairments result from the delocalization of mitochondria and not the loss of ER tethers per se. Future studies should investigate Xin binding partners that are currently unknown but specific to the mitochondrion, sarcoplasmic reticulum or cytoskeleton with the potential to provide additional evidence to support these proposed mechanisms.

Clinical implications

While this work has been conducted in mice, the clinical implications of these findings should not be overlooked. It is estimated that 70-80% of mitochondrial myopathy are the result of mutations to nuclear genes, however the identity of many of these genes remains unknown[54]. One strategy to address this issue has been the identification and functional characterization of proteins encoded by nuclear genes but that are predicted to be localized to the mitochondria[55,56]. For example, the nuclear encoded C17orf89 was recently found to be a regulator of mitochondrial complex I assembly and was implicated in a case of complex I deficiency[56]. Likewise, Xin is a nuclear encoded protein localized to the mitochondria with a function that remains to be fully elucidated. Xin is known to be expressed within human skeletal muscle, although studies within the human population have been limited[57]. Future experiments may uncover interactions between Xin and other mitochondrial proteins, as well as investigate the link between the loss of Xin and metabolic disease, with the potential to establish Xin's role in mitochondrial myopathy.

Overall, this study has demonstrated that Xin-/- mice fed a high fat diet experience dysfunctional whole-body glucose regulation characterized by impaired glucose uptake and elevated fasted blood glucose levels, indicative of overt diabetes. Structural impairments to skeletal muscle mitochondria were also present and were characterized by mitochondrial swelling, streaming and loss of cristae. These structural deficiencies translated into functional mitochondrial impairments, with deficiencies at the level of individual mitochondria. While an increase in mitochondrial content was also noted, there were no differences in the content of autophagy or mitochondrial fission or fusion associated proteins between Xin-/- HFD and WT HFD mice. Future studies should aim to determine the mechanism connecting the loss of Xin to these changes by investigating Xin's potential role as a mitochondrial tether and applying these novel findings to the human population.

References

1. Thiebaud, D. et al. The effect of graded doses of insulin on total glucose uptake, glucose oxidation, and glucose storage in man. Diabetes **31,** 957–963 (1982).

2. DeFronzo, R. A., Gunnarsson, R., Björkman, O., Olsson, M. & Wahren, J. Effects of insulin on peripheral and splanchnic glucose metabolism in noninsulin-dependent (type II) diabetes mellitus. J. Clin. Invest. **76,** 149–155 (1985).

3. Lundby, C. & Jacobs, R. A. Adaptations of skeletal muscle mitochondria to exercise training. Exp. Physiol. **101,** 17–22 (2016).

4. Meinild Lundby, A.-K. et al. Exercise training increases skeletal muscle mitochondrial volume density by enlargement of existing mitochondria and not de novo biogenesis. Acta Physiol (Oxf) **222,** (2018).

5. Sivitz, W. I. & Yorek, M. A. Mitochondrial Dysfunction in Diabetes: From Molecular Mechanisms to Functional Significance and Therapeutic Opportunities. Antioxid Redox Signal **12,** 537–577 (2010).

6. Patti, M. E. et al. Coordinated reduction of genes of oxidative metabolism in humans with insulin resistance and diabetes: Potential role of PGC1 and NRF1. Proc. Natl. Acad. Sci. U.S.A. **100,** 8466–8471 (2003).

7. Mootha, V. K. et al. PGC-1alpha-responsive genes involved in oxidative phosphorylation are coordinately downregulated in human diabetes. Nat. Genet. **34,** 267–273 (2003).

8. He, J., Watkins, S. & Kelley, D. E. Skeletal Muscle Lipid Content and Oxidative Enzyme Activity in Relation to Muscle Fiber Type in Type 2 Diabetes and Obesity. Diabetes **50,** 817–823 (2001).

9. Kelley, D. E., He, J., Menshikova, E. V. & Ritov, V. B. Dysfunction of mitochondria in human skeletal muscle in type 2 diabetes. Diabetes **51,** 2944–2950 (2002).

10. Ritov, V. B. et al. Deficiency of subsarcolemmal mitochondria in obesity and type 2 diabetes. Diabetes **54,** 8–14 (2005).

11. Al-Sajee, D. Investigating the roles of Xin in skeletal muscle and its satellite cell population. (2017).

12. Hancock, C. R. et al. High-fat diets cause insulin resistance despite an increase in muscle mitochondria. Proc. Natl. Acad. Sci. U.S.A. **105,** 7815–7820 (2008).

13. Monaco, C. M. F. et al. Altered mitochondrial bioenergetics and ultrastructure in the skeletal muscle of young adults with type 1 diabetes. Diabetologia **61,** 1411–1423 (2018).

14. Fisher-Wellman, K. H. et al. Mitochondrial glutathione depletion reveals a novel role for the pyruvate dehydrogenase complex as a key H2O2-emitting source under conditions of nutrient overload. Free Radic. Biol. Med. **65,** 1201–1208 (2013).

15. Corcoran, M. P., Lamon-Fava, S. & Fielding, R. A. Skeletal muscle lipid deposition and insulin resistance: effect of dietary fatty acids and exercise. Am. J. Clin. Nutr. **85,** 662–677 (2007).

16. King, A. J. F. The use of animal models in diabetes research. Br. J. Pharmacol. **166,** 877–894 (2012).

17. Li, Y., Xu, S., Zhang, X., Yi, Z. & Cichello, S. Skeletal intramyocellular lipid metabolism and insulin resistance. Biophys Rep **1,** 90–98 (2015).

18. Meex, R. C. R., Schrauwen, P. & Hesselink, M. K. C. Modulation of myocellular fat stores: lipid droplet dynamics in health and disease. Am. J. Physiol. Regul. Integr. Comp. Physiol. **297,** R913-924 (2009).

19. Petersen, K. F., Dufour, S., Befroy, D., Garcia, R. & Shulman, G. I. Impaired mitochondrial activity in the insulin-resistant offspring of patients with type 2 diabetes. N. Engl. J. Med. **350,** 664–671 (2004).

20. Morino, K. et al. Reduced mitochondrial density and increased IRS-1 serine phosphorylation in muscle of insulin-resistant offspring of type 2 diabetic parents. J Clin Invest **115,** 3587–3593 (2005).

21. Jackson, K. C. et al. Ectopic lipid deposition and the metabolic profile of skeletal muscle in ovariectomized mice. Am. J. Physiol. Regul. Integr. Comp. Physiol. **304,** R206-217 (2013).

22. Mizushima, N., Yoshimori, T. & Levine, B. Methods in mammalian autophagy research. Cell **140,** 313–326 (2010).

23. Moore, A. S., Wong, Y. C., Simpson, C. L. & Holzbaur, E. L. F. Dynamic actin cycling through mitochondrial subpopulations locally regulates the fission–fusion balance within mitochondrial networks. Nature Communications **7,** 12886 (2016).

24. Cherepanova, O. et al. Xin-repeats and Nebulin-like Repeats Bind to F-actin in a Similar Manner. Journal of Molecular Biology **356,** 714–723 (2006).

25. Sebastián, D. et al. Mitofusin 2 (Mfn2) links mitochondrial and endoplasmic reticulum function with insulin signaling and is essential for normal glucose homeostasis. PNAS **109,** 5523–5528 (2012).

26. Betz, C. et al. Feature Article: mTOR complex 2-Akt signaling at mitochondria-associated endoplasmic reticulum membranes (MAM) regulates mitochondrial physiology. Proc. Natl. Acad. Sci. U.S.A. **110,** 12526–12534 (2013).

27. Tubbs, E. et al. Mitochondria-associated endoplasmic reticulum membrane (MAM) integrity is required for insulin signaling and is implicated in hepatic insulin resistance. Diabetes **63,** 3279–3294 (2014).

28. Lemasters, J. J., Theruvath, T. P., Zhong, Z. & Nieminen, A.-L. Mitochondrial calcium and the permeability transition in cell death. Biochim. Biophys. Acta **1787,** 1395–1401 (2009).

29. Bravo, R. et al. Increased ER-mitochondrial coupling promotes mitochondrial respiration and bioenergetics during early phases of ER stress. J. Cell. Sci. **124,** 2143–2152 (2011).

30. Arruda, A. P. et al. Chronic enrichment of hepatic ER-mitochondria contact sites leads to calcium dependent mitochondrial dysfunction in obesity. Nat Med **20,** 1427–1435 (2014).

31. Hamasaki, M. et al. Autophagosomes form at ER–mitochondria contact sites. Nature **495,** 389–393 (2013).

32. Gelmetti, V. et al. PINK1 and BECN1 relocalize at mitochondria-associated membranes during mitophagy and promote ER-mitochondria tethering and autophagosome formation. Autophagy **13,** 654–669 (2017).

33. Donohue, E. et al. Inhibition of autophagosome formation by the benzoporphyrin derivative verteporfin. J. Biol. Chem. **286,** 7290–7300 (2011).

34. Lee, H. & Yoon, Y. Mitochondrial fission: regulation and ER connection. Mol. Cells **37,** 89–94 (2014).

35. van Vliet, A. R., Verfaillie, T. & Agostinis, P. New functions of mitochondria associated membranes in cellular signaling. Biochim. Biophys. Acta **1843,** 2253–2262 (2014).

36. Friedman, J. R. et al. ER tubules mark sites of mitochondrial division. Science **334,** 358–362 (2011).

37. de Brito, O. M. & Scorrano, L. Mitofusin 2 tethers endoplasmic reticulum to mitochondria. Nature **456,** 605–610 (2008).

38. Zorzano, A., Liesa, M. & Palacín, M. Role of mitochondrial dynamics proteins in the pathophysiology of obesity and type 2 diabetes. Int. J. Biochem. Cell Biol. **41,** 1846–1854 (2009).

39. Tubbs, E. et al. Disruption of Mitochondria-Associated Endoplasmic Reticulum Membranes (MAMs) Integrity Contributes to Muscle Insulin Resistance in Mice and Humans. Diabetes db170316 (2018).

40. Giorgi, C. et al. PML regulates apoptosis at endoplasmic reticulum by modulating calcium release. Science **330,** 1247–1251 (2010).

41. Bononi, A. et al. Identification of PTEN at the ER and MAMs and its regulation of Ca(2+) signaling and apoptosis in a protein phosphatase-dependent manner. Cell Death Differ. **20,** 1631–1643 (2013).

42. Theurey, P. et al. Mitochondria-associated endoplasmic reticulum membranes allow adaptation of mitochondrial metabolism to glucose availability in the liver. J Mol Cell Biol **8,** 129–143 (2016).

43. Anesti, V. & Scorrano, L. The relationship between mitochondrial shape and function and the cytoskeleton. Biochimica et Biophysica Acta (BBA) - Bioenergetics **1757,** 692–699 (2006).

44. Paulin, D. & Li, Z. Desmin: a major intermediate filament protein essential for the structural integrity and function of muscle. Exp. Cell Res. **301,** 1–7 (2004).

45. Rappaport, L., Oliviero, P. & Samuel, J. L. Cytoskeleton and mitochondrial morphology and function. Mol. Cell. Biochem. **184,** 101–105 (1998).

46. Schwarz, N. & Leube, R. E. Intermediate Filaments as Organizers of Cellular Space: How They Affect Mitochondrial Structure and Function. Cells **5,** (2016).

47. Milner, D. J., Mavroidis, M., Weisleder, N. & Capetanaki, Y. Desmin Cytoskeleton Linked to Muscle Mitochondrial Distribution and Respiratory Function. J Cell Biol **150,** 1283–1298 (2000).

48. Reipert, S. et al. Association of mitochondria with plectin and desmin intermediate filaments in striated muscle. Exp. Cell Res. **252,** 479–491 (1999).

49. Winter, L., Abrahamsberg, C. & Wiche, G. Plectin isoform 1b mediates mitochondrion-intermediate filament network linkage and controls organelle shape. J. Cell Biol. **181,** 903–911 (2008).

50. Eulitz, S. et al. Identification of Xin-repeat proteins as novel ligands of the SH3 domains of nebulin and nebulette and analysis of their interaction during myofibril formation and remodeling. Mol Biol Cell **24,** 3215–3226 (2013).

51. Yamamoto, D. L. et al. The nebulin SH3 domain is dispensable for normal skeletal muscle structure but is required for effective active load bearing in mouse. J. Cell. Sci. **126,** 5477–5489 (2013).

52. Bang, M.-L., Gregorio, C. & Labeit, S. Molecular dissection of the interaction of desmin with the C-terminal region of nebulin. J. Struct. Biol. **137,** 119–127 (2002).

53. Tonino, P. et al. Reduced myofibrillar connectivity and increased Z-disk width in nebulin-deficient skeletal muscle. J. Cell. Sci. **123,** 384–391 (2010).

54. Haller, R. G. & DiMauro, S. Metabolic and Mitochondrial Myopathies. in Muscle 1031–1041 (Elsevier, 2012).

55. Alston, C. L., Rocha, M. C., Lax, N. Z., Turnbull, D. M. & Taylor, R. W. The genetics and pathology of mitochondrial disease. J. Pathol. **241,** 236–250 (2017).

56. Floyd, B. J. et al. Mitochondrial Protein Interaction Mapping Identifies Regulators of Respiratory Chain Function. Mol. Cell **63,** 621–632 (2016).

57. Nilsson, M. I. et al. Xin Is a Marker of Skeletal Muscle Damage Severity in Myopathies. The American Journal of Pathology **183,** 1703–1709 (2013).

58. Bloemberg, D. & Quadrilatero, J. Rapid determination of myosin heavy chain expression in rat, mouse, and human skeletal muscle using multicolor immunofluorescence analysis. PLoS ONE **7,** e35273 (2012).

Appendix

Supplemental Methods

Histochemical staining and analysis

Succinate dehydrogenase (SDH) staining was used to estimate mitochondrial content. Mouse TA muscle samples were sectioned at 8μm and incubated with 0.2M phosphate buffer (pH 7.4), 0.2M sodium succinate and nitroblue tetrazolium (Sigma, N6876) at 37°C for 1 hour. Xin-Tom20 and Xin-desmin co-stains were used to determine the degree of colocalization between Xin and Tom20 and Xin and desmin. Human skeletal muscle tissue samples were sectioned at 8μm and subsequently blocked for 1 hour with 1.5% normal goat serum (NGS). Sections were incubated overnight with Tom20 antibody (1:50, Santa Cruz sc-17764) or for 1 hour with desmin antibody (1:100, Vector Laboratories VP-D502), followed by an overnight incubation with Xin antibody (1:500, Genway 30909-MMU921931). Appropriate Alexa secondary antibodies were applied after each incubation (1:250, Life Technologies A11005, A21131). To determine if Xin expression varies with fibre type, a fibre-type stain was performed and compared to sections stained with Xin. Human skeletal muscle tissue was sectioned at 10μm and stained according to methods developed by Bloemberg and Quadrilatero[58]. For Xin, human skeletal muscle tissue samples were sections at 10μm, blocked for 1 hour with 1.5% normal goat serum (NGS) and incubated overnight with Xin antibody (1:500, Genway 30909-MMU921931). The appropriate Alexa secondary antibody was subsequently applied (1:250, Life Technologies A11005). All imaging and analysis was conducted using a Nikon 90i microscope and Nikon NIS-Elements ND2 software (Melville, NY, USA). Xin-Tom20 and Xin-desmin image deconvolution was performed using Fiji ImageJ.

Western Blot Analysis

Western blot analysis was performed as described above (see section: methods, western blot analysis). The primary antibody total OXPHOS rodent antibody cocktail (1:250, Abcam 110413) was used for analysis of mitochondrial electron transport chain complex content.

Supplemental Figures

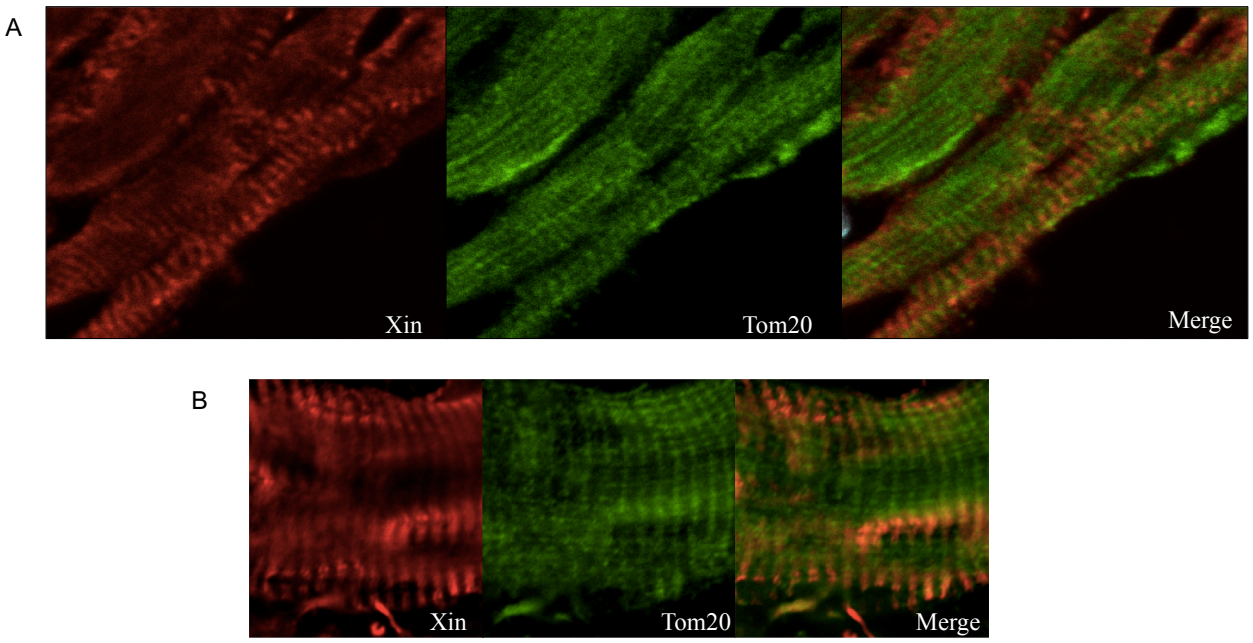

Supplemental Figure 1. Xin partially co-localizes with the mitochondrial protein Tom20. Immunofluorescent stain using anti-Xin and anti-Tom20 antibodies in human gluteal muscle at 60x (A) and 90x (B) magnification shows predominately a transverse striated staining pattern for Xin and transverse and longitudinal striated staining pattern for Tom20. Merged images identify areas of Xin and Tom20 co-localization, shown in yellow, indicating partial co-localization between the two proteins.

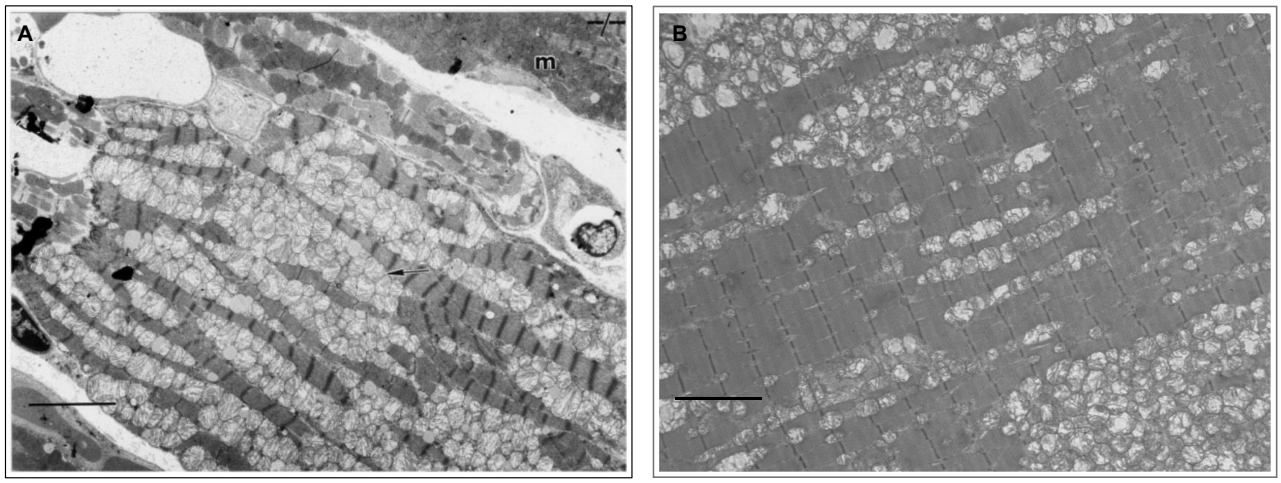

Supplemental Figure 2. Striated muscle mitochondria display similar changes in desmin-/- and Xin-/- mice. Mitochondria within desmin-/- cardiac muscle are swollen and have proliferated throughout the muscle fibre (A). A similar phenotype is seen in Xin-/- skeletal muscle, characterized by an increase in mitochondrial area and content (B). (A) Scale bar = 5μm; (B) Scale bar = 4μm. Image (A) produced by Milner et al., 2000[47].

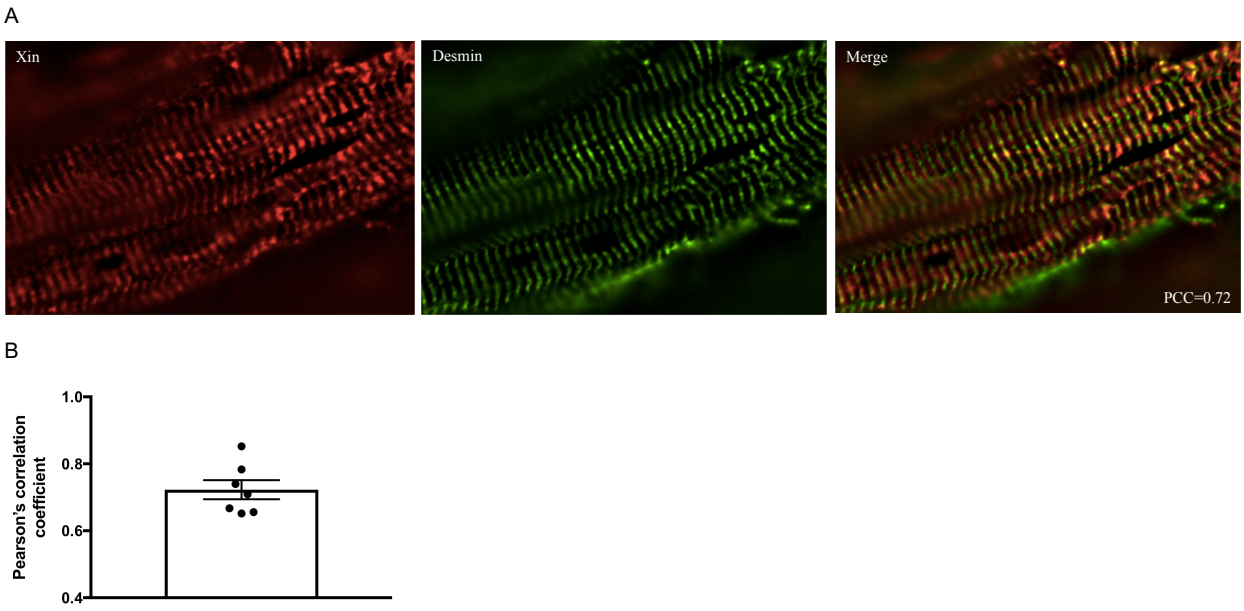

Supplemental Figure 3. Xin and desmin display a partial co-localization in skeletal muscle. Immunofluorescent staining using anti-Xin and anti-desmin antibodies in human gluteal muscle at 60x magnification shows areas of partial co-localization between Xin and desmin, indicated by yellow fluorescence in the merged imaged. Further analysis identified a Pearson's correlation coefficient (PCC) of 0.72 (B). N=7 images from 2 samples.

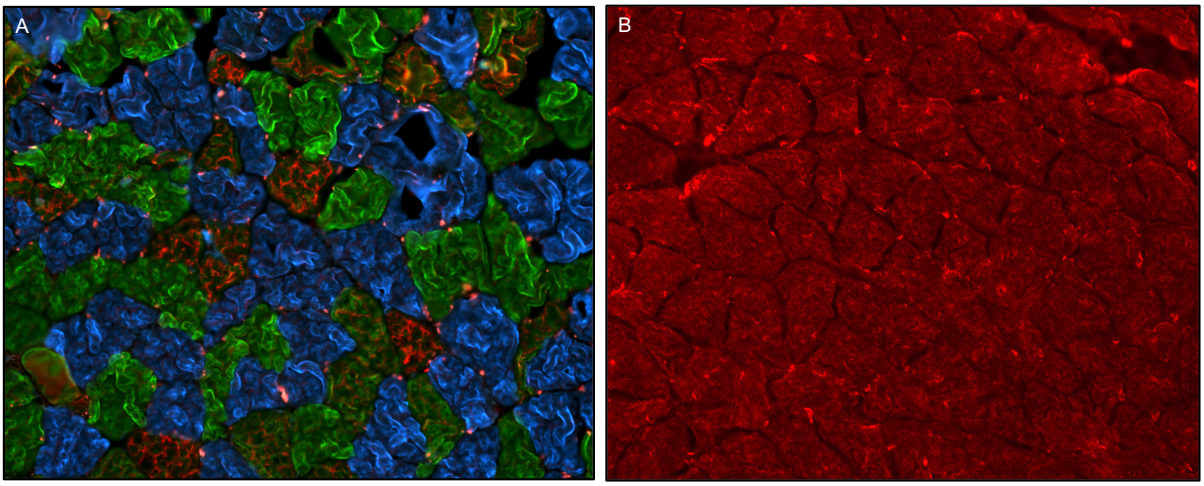

Supplemental Figure 4. Xin expression is not fibre-type specific. (A) Human gluteal muscle exhibits a mosaic pattern of fibre-type expression made up of type 1 (blue), type IIa (green) and type IIx (red) fibres. (B) Xin expression is unaffected by fibre-type, as staining is consistent throughout all fibre types.

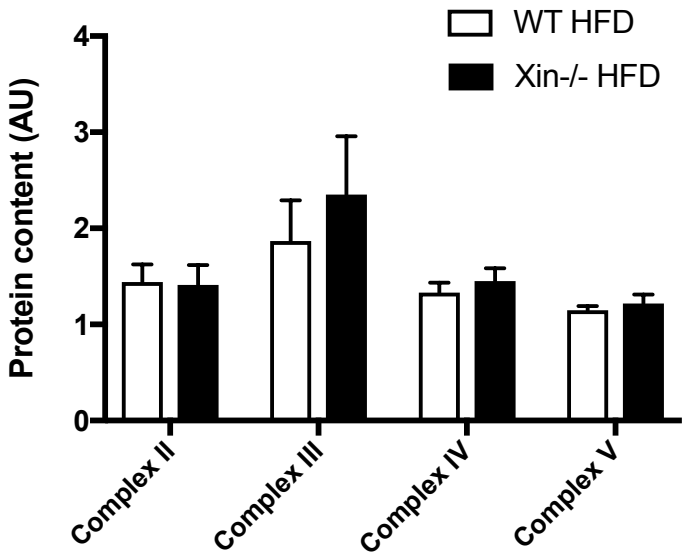

Supplemental Figure 5. Xin-/- HFD and WT HFD mice experienced no difference in the protein content of mitochondrial oxidative phosphorylation complexes. Analysis of western blots for the mitochondrial OXPHOS complexes II-V revealed no differences in the content of any protein complex between Xin-/- HFD and WT HFD mice. Values represent mean ± SEM. *P < 0.05. N=9-12/group.

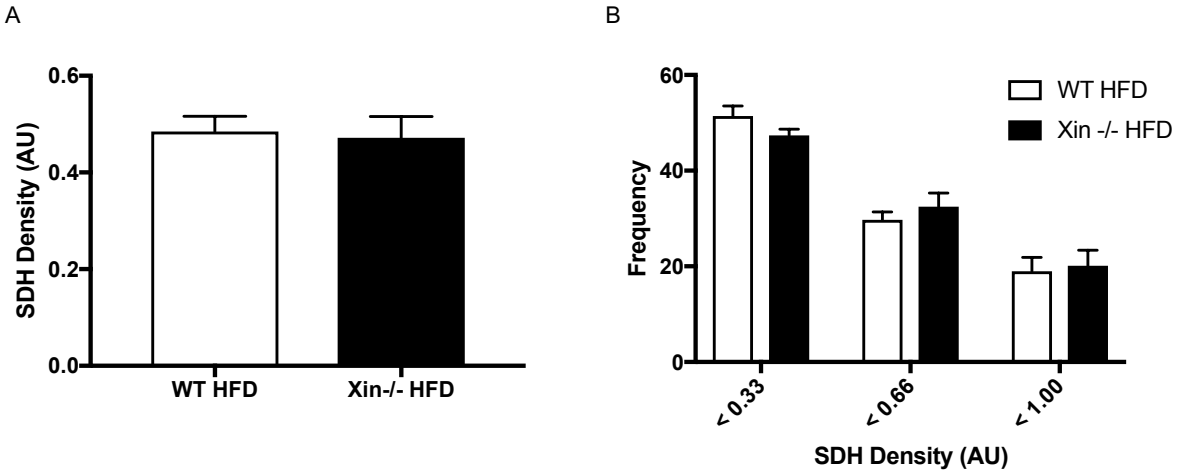

Supplemental Figure 6. Xin-/- HFD and WT HFD mice displayed no difference in the density of succinate dehydrogenate (SDH) stain. Analysis of Xin-/- HFD and WT HFD TA muscle revealed no difference in the average SDH stain density between the two groups, suggesting no difference in mitochondrial content (A). There was also no difference in the frequency of fibres stained at various densities of SDH stain (B).